



Last Glacial ice-sheet dynamics offshore NE Greenland – a case study from Store Koldewey Trough

Ingrid L. Olsen¹, Matthias Forwick¹, Jan Sverre Laberg¹, Tom Arne Rydningen¹, Katrine Husum²

¹Department of Geosciences, UiT The Arctic University of Norway, Box 6050 Langnes, NO-9037 Tromsø, Norway

²Norwegian Polar Institute, Box 6606 Langnes, NO-9296 Tromsø, Norway

Correspondence to: Ingrid L. Olsen (ingrid.l.olsen@uit.no)

Abstract

New swath bathymetry and high-resolution seismic data, supplemented with multi-proxy analyses of sediment gravity cores from Store Koldewey Trough, NE Greenland, support the presence of a shelf-break terminating Greenland Ice Sheet (GIS) on the northeastern part of the Greenland Margin during the Last Glacial Maximum (LGM). The presence of mega-scale glacial lineations and a grounding zone wedge in the outer part of the trough provides evidence of the expansion of fast-flowing, grounded ice, probably originating from the area presently covered with the Storstrømmen ice stream and cutting across Store Koldewey Island and Germania Land. Multiple halts and/or readvances interrupted the deglaciation. Two sets of crevasse-squeezed ridges in the outer and middle part of the trough may indicate repeated surging of the GIS during the deglaciation. The complex landform assemblage in Store Koldewey Trough is suggested to reflect a relatively slow and stepwise retreat during the deglaciation. Thus, the ice retreat probably occurred asynchronously relative to other ice streams offshore NE Greenland. Subglacial till fills the trough, with an overlying thin drape of maximum 2.5 m thickness of glacier proximal and glacier distal sediment. At a late stage of the deglaciation, the ice stream retreated across Store Koldewey Island and Germania Land, terminating the sediment input from this sector of the GIS to Store Koldewey Trough.

1 Introduction

The Greenland Ice Sheet (GIS) is the second largest ice sheet on Earth storing 2.9 million km³ of ice (Dahl-Jensen et al., 2009). The GIS has been exposed to increasing ice loss during the last decades, contributing 0.6 ± 0.1 mm/yr to global sea-level rise between 2000-2010 (Fürst et al., 2015). About 16% of the GIS are presently drained via marine terminating outlet glaciers in NE Greenland, mostly through the North East Greenland Ice Stream (NEGIS) (Joughin et al. 2000) consisting of three main outlets: 79°-Glacier, Zachariae Isstrøm and Storstrømmen (e.g. Rignot and Kanagaratnam 2006) (Fig. 1). A future warming global climate, which will be particularly strong in the Arctic (Serreze and Francis, 2006), will lead to a reduced sea-ice cover adjacent to the glacier termini and subsequent accelerated melting of the ice sheet in NE Greenland (Bendtsen et al., 2017). Thus, a continuing global warming could cause an instability and possibly irreversible loss of the GIS, which has - together with the West-Antarctic Ice Sheet (WAIS) - been identified as tipping elements in the Earth's climate system (Lenton et al., 2008). A complete meltdown of these ice sheets can potentially lead to a global sea-level rise of 7.3 (GIS) m and 3.2 m (WAIS) (Bamber et al., 2001, 2009), causing severe consequences for coastal societies (IPCC, 2018). However, precise predictions of the evolvement of a potential decay of the GIS in the future remains difficult (Nick et al., 2013). By getting a better understanding of the development of glaciers in response to past climate changes, e.g. from the Last Glacial Maximum (LGM; c. 24-16 ka BP) and up to present, we contribute to validation and improvement of numerical models focusing on present processes, as well as the future development of glaciers and ice sheets.



The reconstruction of the GIS configuration and dynamics from marine-geoscientific data, including maximum extent during the LGM, as well as the timing and dynamics of the deglaciation, have been addressed in multiple studies (e.g. Dowdeswell et al. 1994; Hubberten et al. 1995; Andrews et al. 1998; Bennike et al. 2002; Funder et al. 2011; Hogan et al. 2011; Ó Cofaigh et al. 2013; Hogan et al. 2016). However, these reconstructions focus primarily on the southern and western sectors offshore Greenland, and reconstructions from offshore northeast Greenland remain sparse (Arndt, 2018; Arndt et al., 2017; Evans et al., 2002; Laberg et al., 2017; Stein et al., 1996; Winkelmann et al., 2010). It has been suggested that the northeastern part of the GIS reached the inner or middle parts of the continental shelf during its maximum extent during the last glacial (see Funder et al. 2011 for a review). However, subglacial and ice-marginal depositional landforms, including mega-scale glacial lineations and recessional moraines presented in more recent marine geoscientific studies suggest that the northeastern sector of the GIS extended all the way to the shelf edge during the last glacial (Arndt, 2018; Arndt et al., 2017; Laberg et al., 2017).

Laberg et al. (2017) presented glacial landforms interpreted as retreat moraines in the outer parts of the Store Koldewey Trough (Fig. 1), suggesting a stepwise early deglaciation likely triggered by an increase in ocean temperature. However, an absolute chronology for the deglaciation is still pending. According to Evans et al. (2002), breakup and retreat of the GIS further to the south, outside Kejser Franz Joseph Fjord (for location, see Fig. 1), commenced after c. 15.3 ka BP, with the ice abandoning the mid-shelf before 13 ka BP and the inner shelf being ice free before 9 ka BP. Dating of lake sediments on Store Koldewey Ø, located east of Store Koldewey Trough (Fig. 1), reveal that the area was deglaciated prior to 11 ka BP (Klug et al., 2009), whereas the ice front rested east of the present coastline of Germania Land until c. 10 ka BP (Landvik, 1994). By 7.5 ka BP the ice front had retreated close to its present position, and after further recession Germania Land became an island about 6 ka BP. Storstrømmen readvanced again c. 1 ka BP, reaching its present position during the Little Ice Age (Weidick et al., 1996).

The overall objective of this paper is to confirm the presence of a shelf-break terminating GIS on the northeastern part of the Greenland Margin by presenting evidence from new acoustic data (multibeam bathymetry and Chirp seismic) and sediment cores. Furthermore, the aims are to 1) reconstruct the ice dynamics and ice drainage pathways of this sector of the GIS overlying Store Koldewey Trough during the LGM and the deglaciation, and 2) discuss the post-glacial marine environmental conditions of Store Koldewey Trough, one of the largest glacial troughs offshore northeast Greenland.

2 Regional setting

The large-scale morphology of the NE Greenland continental shelf is characterized by several large cross-shelf troughs separated by shallower banks and shoals (Fig. 1). The troughs are characteristic features of formerly glaciated continental shelves, interpreted as glacially over-deepened landforms acting as conduits for fast-flowing ice streams eroding into the sub-glacial bedrock (e.g. Vorren et al. 1988; Canals et al. 2000; Batchelor and Dowdeswell 2014), whilst inter-trough banks are interpreted to have been covered by slower flowing ice, consequently experiencing less erosion (Klages et al., 2013; Ottesen and Dowdeswell, 2009).

The east coast of Greenland is presently largely influenced by the southward flowing East Greenland Current carrying cold and fresh surface Polar Water and sea ice from the Arctic Ocean together with warmer modified Atlantic Intermediate Water (Aagaard and Coachman, 1968; Hopkins, 1991). An increased inflow of warm Atlantic Intermediate Water into East Greenland troughs and fjords is thought to influence the submarine melt rates, causing an instability at the grounding line of marine terminating outlet glaciers (Khan et al., 2014; Mayer et al., 2018), e.g. the 79°-Glacier (Straneo and Heimbach, 2013; Wilson and Straneo, 2015).

Store Koldewey Trough is a NW-SE oriented cross-shelf trough located ~76° N offshore northeast Greenland (Fig. 1). The trough is ~210 km long, 30-40 km wide, up to 400 m deep. It has a sinuous centerline terminating at the shelf edge. A bathymetric profile along the axis of Store Koldewey Trough reveals that it differs from most troughs



offshore northeast Greenland, it is a seaward deepening trough (Fig. 1B). In addition, Store Koldewey Trough is the only trough on the NE Greenland continental shelf without a fjord continuation; it terminates near Germania Land and the island Store Koldewey to the west (Fig. 1A).

5 The ice stream Storstrømmen, located west of the study area (Fig. 1), has presently a floating ice tongue with a 20 km wide calving front (Khan et al., 2014). It surged around 1910 and 1978 (Mouginot et al., 2018). Similar to surging glaciers on Svalbard (e.g. Dowdeswell et al., 1991), Storstrømmen undergoes a slow initiation and termination with a long active surge phase lasting 10 years (Mouginot et al., 2018). The bed topography beneath the ice stream has a reverse slope, resulting in accumulation of subglacial water creating favorable conditions for surges (Mouginot et al., 2018), as well as episodically calving events (Hill et al., 2018).

Gneisses from the Caledonian fold belt of East Greenland as well as Mesozoic and Cenozoic marine deposits dominate the bedrock geology of the drainage area of Storstrømmen (Henriksen and Higgins, 2009; Koch, 1916).

15 Laberg et al. (2017) identified an assemblage of glacial landforms in the outer part of Store Koldewey Trough, including mega-scale glacial lineations and rhombohedral- and transverse ridges with variable dimensions. From the landform assemblage, it was inferred that grounded ice expanded to the shelf edge during the last glacial. Four prominent transverse ridges located on the outer, middle and inner shelf were interpreted as grounding-zone wedges deposited in front of the GIS during temporary stillstand and/or readvances during the last deglaciation (see labels A-D in Fig. 1B, C). Similar landform assemblages are also identified in other troughs along the northeastern continental shelf of Greenland (Arndt, 2018; Arndt et al., 2015) as well as on other formerly glaciated continental shelves (e.g. Ottesen et al. 2005; Winsborrow et al. 2010; Jakobsson et al. 2012a; Bjarnadóttir et al. 2013; Andreassen et al. 2014; Batchelor and Dowdeswell 2014).

25 3 Material and methods

Acoustic data, including swath bathymetry and high-resolution seismic data, as well as four sediment gravity cores were collected during cruises arranged within the TUNU-program (Christiansen, 2012) using *R/V Helmer Hanssen* in 2013, 2015 and 2017.

30 The swath bathymetry data was acquired using hull-mounted Kongsberg Maritime Simrad EM 300 and 302 multibeam echo sounders in 2013/2015 and 2017, respectively. Sound velocity profiles for the water column were derived from CTD measurements prior to and during the bathymetric surveys. High-resolution seismic profiles were acquired with a hull-mounted EdgeTech 3300-HM (Chirp) sub-bottom profiler simultaneously with the swath bathymetry data, using a pulse frequency of 2-8 kHz. Visualization and interpretation of the chirp and multibeam bathymetry data were performed using Petrel 2018 and Global Mapper 19.

35 The sediment gravity cores (HH17-1326, HH17-1328, HH17-1331 and HH17-1333) were retrieved from 294 to 345 m water depth along a transect extending from inner to middle Store Koldewey Trough using a 6 m long steel barrel (Fig. 1; Table 1). Coring sites were chosen with the purpose of penetrating a stratigraphic sequence including subglacial and glacial marine deposits.

40 Prior to opening, the physical properties of the sediments were measured using the GEOTEK Multi Sensor Core Logger, with a 10 mm step size and 10 s measuring time. The cores were stored for one day in the laboratory prior to the measurements to allow the sediments to adjust to room temperature as temperature changes can affect the physical properties (Weber et al., 1997). After splitting, color images were acquired with a Jai L-107CC 3 CCD RGB Line Scan Camera installed on an Avaatech XRF core scanner. Furthermore, X-radiographs were taken with a GEOTEK MSCL-XCT X-ray core imaging system. X-Ray Fluorescence (XRF) core scanning for qualitative element-geochemical analyses using an Avaatech XRF Core Scanner was performed. The data acquisition was carried out in 10 mm measurement steps in two runs with a 12 mm cross-core slit size and following settings; 1) 45 10 kV, 1000 μ A, 10 sec counting time and no filter; 2) 30 kV, 2000 μ , 10 sec counting time and Pd-thick filter.



XRF return values for Ca, Fe and Ti divided over the sum of the most abundant elements (Al, Si, K, Ca, Ti, Fe and Rb) were chosen for further interpretation, recording the relative variations in marine carbonate/detrital input and terrigenous sediment delivery. In addition, a systematic description of the sediment surface was carried out and colors were determined visually using the Munsell Soil Color Chart (Munsell, 2000). Shear strength of the sediments were estimated using the fall-cone test (Hansbo, 1957).

Grain-size analyses were performed using a Beckman Coulter LS 13 320 laser particle size analyzer, measuring the range from 0.04 μm to 2000 μm . Particles larger than 2000 μm were removed by a sieve and are presented as clasts in the lithological logs. Prior to the analyses, chemical treatment of the samples using HCl and H₂O₂ were conducted to remove carbonates and organic content, respectively. Distilled water was added to the samples before being shaken for 24 hours. Furthermore, two drops of Calgon solution were added to the samples before being placed in an ultrasound bath for five minutes in order to disintegrate flocculation of particles. Each sample was analyzed three times and the particle size statistics were calculated using GRADISTAT v. 8.0 (Blott and Pye, 2001).

4 Results

4.1 Lithostratigraphy of the uppermost trough strata

Five lithofacies are defined based on the lithological composition, sedimentary structures, physical properties and sediment geochemistry (Fig. 2 and 3). The properties of the different facies are summarized in Table 2.

4.1.1 Facies 5 - Diamicton (Dmm)

The lowermost facies in all four cores comprises a very dark gray, massive, matrix-supported diamicton with a sandy mud matrix and high amounts of randomly oriented clasts of various origin (Fig. 2 and 3; Table 2). The upper boundary is sharp and bioturbation is absent. Both the magnetic susceptibility and Ca/Sum ratio vary between each core, with the highest in HH17-1326 and lowest in HH17-1328. Wet bulk density and shear strength values are generally high, suggesting over-consolidation of the sediments.

Based on the poorly sorted nature of these deposits, the high amounts of clasts, absence of bioturbation and a considerable consolidation of the sediments we suggest that the facies represents diamictic subglacial debris/basal till deposited at the base of an ice stream from the GIS (compare with Evans et al. 2006). The facies is recognized in the seismostratigraphy as an acoustically transparent unit (Fig. 7).

4.1.2 Facies 4 – Interlaminated glacimarine sediments (FI)

Facies 4 is present in the two westernmost cores; HH17-1326 and HH17-1328, with thicknesses of 12 cm and 35 cm, respectively (Fig. 2 and 3, Table 2). The facies consists of dark gray laminated mud with fine sandy layers. Bioturbation and clasts are absent. The upper unit boundary is gradational and defined by the onset of dropstone deposition. Wet bulk density is medium, whilst the shear strength and magnetic susceptibility vary with a decrease in HH17-1326 and an increase in HH17-1328 relative to the underlying unit. The measured increase in the shear strength in core HH17-1328 is likely a result of influence of the sandy laminae, causing too high values (Hansbo, 1957). Ti/Sum and Fe/Sum ratios correlate with the sediment grain-size, with higher Fe and Ti content within the sand and mud laminae, respectively.

The facies is interpreted to contain glacier-proximal glacimarine sediments deposited as emanating subglacial meltwater at the grounding line generates two coupled density currents: suspension plumes transporting fine-grained sediments and high-density underflows (hyperpycnal flows; Mulder et al. 2003) carrying coarser



5 sediments. The lack of clasts interpreted as ice-rafted debris (IRD) in ice-proximal settings may have several explanations; i) the time of deposition may represent a period with an extensive sea-ice cover preventing icebergs to drift over the area (Jennings and Weiner, 1996; Moon et al., 2015; Vorren and Plassen, 2002), ii) the sediments may be deposited in a sub-shelf environment proximal to the grounding line (Jennings et al., 2019) or iii) as a result of a high flux of sediment-laden glacial meltwater masking the amount of iceberg rafted debris (Boulton, 1990).

4.1.3 Facies 3 – Interlaminated glacimarine sediments with occasional IRD (F1 (d))

10 Facies 3 occurs in all sediment cores. It consists of dark gray laminated mud with fine sandy layers and clasts (Fig. 2 and 3; Table 2). The clasts, interpreted as IRD, appear in layers. The unit is 9-23 cm thick and has a sharp or gradational lower boundary overlying either facies 5 or 4, respectively, whilst the upper boundary is gradational. The unit has similar properties as facies 4, with medium-high wet bulk density and varying shear strength. However, the magnetic susceptibility varies between the cores.

15 Facies 3 is interpreted to represent a glacier-proximal setting with glacimarine sediments containing IRD deposited rapidly in periods of high calving rates (e.g. Ó Cofaigh and Dowdeswell 2001). The sediments are thought to have been deposited in more open conditions with more intense iceberg rafting compared to facies 4, possibly reflecting an outer ice-proximal setting where IRD becomes a more dominant component (cf. Boulton 1990).

20 4.1.4 Facies 2 – Massive glacimarine sediments (Fm)

Massive olive gray to dark gray mud with little to moderate bioturbation and rare clasts composes facies 2. The facies is 10-80 cm thick and occurs in all four sediment cores (Fig. 2 and 3; Table 2). Both the lower and upper unit boundaries are gradational. The physical properties, including wet bulk density, magnetic susceptibility and shear strength vary slightly within the facies and between the studied sediment cores.

25 The facies is interpreted to reflect suspension settling in an ice-distal glacimarine environment with limited iceberg or sea-ice rafting (Boulton and Deynoux, 1981). However, it could also be speculated that there was a permanent sea ice cover during the deposition of this facies.

30 4.1.5 Facies 1 – Massive glacimarine sediments with IRD (Fm (d))

The uppermost facies in all of the studied cores consists of massive mud with intervals containing clasts, the latter interpreted to be IRD (Fig. 2 and 3; Table 2). The sediment color alternates between brown to dark grayish brown, as well as olive gray to dark olive gray. Facies 1 is generally coarser than facies 2, with a peak in the magnetic susceptibility and decreases in Ti/Sum ratios corresponding to the depth with highest abundance of coarser material. The Ca/Sum ratios increase towards the top of the facies. Both the wet bulk density and shear strength are similar to the underlying facies 2.

35 Facies 1 is interpreted to have been deposited in a similar environment as facies 2. However, the enhanced presence of clasts indicates an increased influence of drifting icebergs and/or sea-ice.

40 4.2 Submarine landforms: glacial – deglacial ice-sheet dynamics

The swath bathymetry data from the middle and outer part of Store Koldewey Trough reveal glacial landforms interpreted to reflect various stages of ice-sheet extent, flow dynamics and retreat patterns.

45 4.2.1 Streamlined landforms – mega-scale glacial lineations (MSGL)



Streamlined trough-parallel grooves and ridges occur in the middle and outer trough (Fig. 4, 5 and 6), terminating close to the shelf edge. Individual ridges have widths of 150-500 m and reliefs between 4-8 m (Table 3). The grooves and ridges are partly eroded and/or overprinted by other landforms, which makes it difficult to measure their lengths. However, they appear to be >1.5 km long with elongation ratios of the ridges generally exceeding 10:1. The landforms occur in clusters with spacing from 200 to 700 m. High-resolution seismic data show that the ridges are acoustically transparent, a property that is characteristic for basal till (Ó Cofaigh et al., 2007) (Fig. 7F).

Based on the spatial distribution, dimensions and orientations, we interpret the grooves and ridges as mega-scale glacial lineations (MSGLs) formed subglacially at the base of a fast-flowing, grounded ice stream (Clark, 1993; King et al., 2009; Spagnolo et al., 2014) draining towards the shelf break. Similar landforms have been described on the seafloor of other formerly glaciated margins where they have been interpreted to indicate the presence of grounded ice streams (e.g. Canals et al. 2000; Ottesen et al. 2005; Evans et al. 2009; Rydningen et al. 2013; Andreassen et al. 2014; Hogan et al. 2016; Arndt 2018).

4.2.2 Large transverse ridges - Grounding zone wedges

Four prominent bathymetric sills interpreted as grounding zone wedge *A-D* by Laberg et al. (2017) are present within the trough (Fig. 1B, C). The wedges are 35-100 m high, 3.5-10 km wide and are spaced 45-60 km apart (Table 3). The cross-trough extent of the grounding zone wedges exceed the multibeam data coverage. Smaller ridges overprint the grounding zone wedges (Fig. 4, 5 and 6A). These large landforms are produced by accumulation of sediments at the ice stream's grounding line, recording the temporary position of the grounding line during stillstand and/or readvance during a late phase of the last glacial (Laberg et al., 2017).

4.2.3 Small ridges – recessional moraines and crevasse-squeeze ridges

The most prominent characteristic of the seafloor throughout Store Koldewey Trough is the high number of small ridges (Fig. 4, 5, 6 and 7). These ridges are one order of magnitude smaller than the grounding-zone wedges and occur in two forms; (1) as curvilinear to straight transverse/semi-transverse ridges, or (2) as rhombohedral ridge patterns. The ridges are up to 2200 m wide, have reliefs <50 m and have a spacing of 50-500 m (Table 3). Some of the ridges superimpose others, implying several generations of ridges. The transverse ridges located southeast of grounding zone wedge *C* appear to be spaced further apart and/or are less well preserved.

We interpret the curvilinear to straight ridges as recessional moraines formed at the grounding line during slow retreat with repeated stillstand and/or small readvances (Dowdeswell et al., 2008; Ó Cofaigh et al., 2008). The rhombohedral network of ridges are interpreted to be crevasse-squeeze ridges that formed from soft sediments squeezed into basal crevasses of the ice stream during and after its transition from fast flow to stagnation, often associated with glacial surges (Boulton et al., 1996; Dowdeswell and Ottesen, 2016; Evans and Rea, 1999; Sharp, 1985; Solheim, 1991). The ridge-like features identified on the sub-bottom profiles are acoustically transparent suggesting a diamictic composition (Stewart and Stoker, 1990) (Fig. 7).

4.2.4 Multi-keel iceberg ploughmarks

Linear to curvilinear depressions with berm ridges along their lateral margins characterize the seafloor east of grounding zone wedge *B* and *C* (Fig. 4, 6B, E and 7D). The depressions are flat-bottomed and occur often in groups. Individual depressions with associated ridges are up to 1.3 km long, 170-1100 m wide and have a relief of 5-30 m (Table 3). They are predominantly orientated parallel to the trough axis. The depressions partly superpose and thereby obscure the underlying transverse ridges and create a chaotic seafloor pattern.

We interpret these landforms as plough marks generated from grounded icebergs with multiple keels. The groups with parallel ploughmarks are comparable to the features suggested to be a result of multi-keeled icebergs in e.g. West-Antarctica (Wise et al., 2017) and northern Barents Sea (Andreassen et al., 2014). However, the ploughmarks



in this study are one magnitude shorter and corrugation ridges within the furrows appear to be absent. We suggest both the uniform orientation and limited length of the ploughmarks to be a result of the presence of an ice mélange limiting iceberg drift, similar to the observations of similar landforms by Kristoffersen et al. (2004) in the Arctic Ocean.

5

4.2.5 Channels

Two straight incisions that are U-shaped in cross section, 150-300 m wide and with incision depths of 3-10 m are identified along the northern and southern trough sidewalls (Fig. 4; Table 3). The incisions are oriented parallel to the recessional moraines and continue beyond the extent of the swath bathymetry data set. They cut into the mega-scale glacial lineations and the acoustically transparent sediments interpreted as basal till. The landforms are interpreted as channels formed during deglaciation as the ice sheet disintegrates and produces fractures filled with meltwater eroding beneath the ice sheet. Another possible explanation for their formation is they could have formed from meltwater runoff from ice masses remaining on the surrounding banks.

10

15 4.3 Seismostratigraphy

Two seismic units (S1 and S2) were identified in the chirp sub-bottom profiles in Store Koldewey Trough (Fig. 7).

4.3.1 Unit S1 – Glacigenic deposits and/or bedrock

20 Seismic unit S1 is the lowermost seismostratigraphic unit and the acoustic basement occurring in the entire study area. It has an acoustically transparent to semi-transparent signature and an irregular top reflection with medium to high amplitude and continuity (Fig. 7B).

25 The unit correlates with lithological unit 5 (*Dmm*) in the sediment cores, interpreted as subglacial till, i.e. that it includes subglacial deposits. However, the chirp profiles (Fig. 7) reveal that the unit S1 also includes grounding-zone wedges, as well as transverse and rhombohedral ridges, i.e. multiple glacigenic landforms and deposits. In the majority of the study area, these glacigenic landforms define the acoustic basement. However, a relatively strong and smooth reflection can be observed beneath glacigenic deposits. This is interpreted to be caused by the top of the underlying bedrock, suggesting that S1 also includes bedrock in some areas.

30

4.3.2 Unit S2 – Latest Weichselian - Holocene glacimarine sediments

Unit S2 is an acoustically transparent unit (Fig. 7). The unit is thin or missing from most of Store Koldewey Trough, with a maximum thickness of 2.5 m where present (Fig. 7). The sediment unit occurs locally either as an infill between the topographic highs or draping the underlying unit S1.

35

Unit S2 is sampled with all four sediment cores and is interpreted to include lithological units 4 (*Fl*), 3 (*Fl (d)*), 2 (*Fm*) and 1 (*Fm (d)*). The unit is identified as glacimarine, consisting of a gradual transition from proximal glacimarine sediments from the latest Weichselian at the base to distal glacimarine Holocene sediments at the top.

40 5 Discussion

5.1 Maximum ice sheet extent and influence of subglacial topography

45 Mega-scale glacial lineations and their termination at grounding zone wedge A in the outer trough (Fig. 5 and 9: Stage 1) suggest that a grounded, fast-flowing ice stream draining the northeastern sector of the GIS extended to the shelf break during the LGM (Fig. 8). This is conform with reconstructions of shelf-break terminating glaciers



during the LGM elsewhere on the NE Greenland Margin, i.e. ranging from our study area in the south to the Westwind Trough at 80.5° N in the north (Arndt et al., 2015, 2017; Laberg et al., 2017; Winkelmann et al., 2010). If the full-glacial conditions on the margin occurred synchronously, this implies that an ice sheet front covered a length of 680 km along the outer shelf.

5

We propose that the Store Koldewey Trough was filled by grounded ice originating from the area presently covered with the Storstrømmen ice stream (Fig. 8A). This implies that the northeastern sector of the GIS reached a thickness allowing the ice stream to flow unrelated to the underlying topography, including the mountain ranges between present day Storstrømmen and Germania Land. Such “pure” ice streams (Bentley, 1987; Stokes and Clark, 1999), flowing unrelated to topography, are documented from the contemporary Siple Coast Ice Streams of West Antarctica. In addition, a similar flow feature has been identified in modern northeast Greenland (Fahnestock et al., 1993), as well as for a paleo-ice stream within the Laurentide Ice Sheet (Cofaigh et al., 2010). Once a fast-flowing ice stream reach deep troughs, they become influenced by topography and stabilize between areas of slower moving ice (Boulton et al., 2003).

10

15

An alternative interpretation is that Store Koldewey Trough had a much smaller drainage-basin, limited to Germania Land (Arndt et al., 2015). However, based on our data, including the observations of mega-scale glacial lineations, recessional moraines and grounding zone wedges, we favor the interpretation of Storstrømmen filling Store Koldewey Trough during full glacial conditions based on the volume of ice needed to fill a trough of this magnitude. We propose that the ice sheet thinned and that the underlying topography controlled the direction of ice flow during a late phase of the last glacial, i.e. that the ice flow from the interior of the GIS was directed to Jøkelbugten in the north and Dove Bugt in the south (Fig. 8B).

20

Acoustic profiles reveal a thin drape of glaciomarine sediment (<2.5 m thick) overlying the glacial deposits in certain parts of the inner and middle trough, whereas a detectable postglacial sediment drape in the outer trough is absent (Fig. 5). Lithofacies Dmm (diamict; subglacial debris/basal till) occurring as the lowermost units in all sediment cores provides supporting evidence that grounded ice from the GIS extended at least to the location of core HH17-1333. Laberg et al. (2017) argue that the lack of postglacial sediments and good preservation of glacial landforms in the outer trough indicate that the identified landforms formed during the LGM and subsequent deglaciation. Stein et al. (1996) presented sediment data from the continental slope off NE Greenland, suggesting that the maximum late Weichselian ice extent occurred at about 21-16 ka BP. Radiocarbon dates from the Greenland Basin indicate that mass-wasting activity on the upper continental slope took place predominantly under full glacial and deglacial conditions and had ceased after about 13 ka BP, leaving the channels largely inactive (Ó Cofaigh et al., 2004). Thus, from the data available, the outer parts of Store Koldewey Trough may have been ice covered in the period from ~21 ka BP - ~13 ka BP.

25

30

35

5.2 Glacial dynamics during deglaciation

The presence of four large grounding zone wedges and recessional moraines indicate that multiple halts and/or readvances interrupted the deglaciation (Fig. 10). The occurrence of such landforms demonstrate a slow retreat of a grounded ice margin accompanied by episodes of longer stillstands (Dowdeswell et al., 2008; Ó Cofaigh et al., 2008). The ice margin must have remained relatively stable for a sufficient period and/or had a considerable sediment flux rate to build large sedimentary depocenters.

40

We interpret the break-up and retreat of the GIS to have happened in two stages; initial retreat by breaking up and calving of grounded ice due to eustatic sea level rise caused by melting of ice at lower latitudes (Lambeck et al., 2014) (Fig. 9: Stage 2) and a second phase of melting driven by ocean warming, possibly due to the onset of inflow of intermediate water masses. The latter is supported by the occurrence of meltwater-channels and laminated sediments interpreted to be a result of excessive meltwater production in the middle and inner parts of the trough.

45



5 There are several factors that possibly can have led to the complex geomorphology in Store Koldewey Trough: i) local highs in an overall shallowing landward seafloor may have provided pinning points, causing ice stabilization and promoting longer stillstands during the deglaciation; ii) though narrowing towards the coast increased lateral stress on the retreating ice margin, thus slowing down/stabilizing it; iii) repeated advances due to glacial surges during deglaciation based on the documented grounding zone wedges *A* and *B* accompanied by crevasse-fill ridges; or iv) the GIS in Store Koldewey Trough had a more dynamic response to the changing climatic and oceanographic conditions compared to troughs of similar dimensions elsewhere on the NE Greenland Margin.

10 Whereas many paleo-ice streams on other glaciated continental shelves with reverse bed slopes experienced a lift-off from the seafloor and an initial rapid retreat due to sea-level rise, e.g. Norske Trough (Arndt et al., 2017), Amundsen Sea in West Antarctica (Smith et al., 2011) and NW Fennoscandian ice sheet (Rydningen et al., 2013)), the ice stream in Store Koldewey Trough stayed grounded or repeatedly stabilized as the trough shallows towards the coast. Consequently, Store Koldewey Trough has a more complex landform assemblage than other ice stream settings on formerly glaciated continental shelves (Fig. 10).

15 The locations and dimensions of grounding zone wedges on the NE Greenland continental shelf have up to recent years been poorly documented. Batchelor and Dowdeswell (2015), referring to Dowdeswell and Fugelli (2012), mention six grounding zone wedges in Store Koldewey Trough based on IBCAO data. However, our data provides evidence for the existence of only four GZW. Large grounding zone wedges have been documented from other cross-shelf troughs in the region (Arndt, 2018; Arndt et al., 2015, 2017; Evans et al., 2002; Winkelmann et al., 2010). These studies reveal, however, the occurrence of only single grounding zone wedges, e.g. in Norske Trough and Westwind Trough (Arndt et al., 2015; Winkelmann et al., 2010). Arndt et al. (2017) suggest that the grounding zone wedges in Norske Trough and Westwind Trough formed as the GIS readvanced during the Younger Dryas. Based on the varying numbers of GZW's we suggest that retreat/readvances of the ice streams offshore NE Greenland occurred asynchronously.

20 The present sub-glacial topography of Storstrømmen consists of a reversed bed slope, accompanied by a floating ice tongue (Hill et al., 2018). Thus, a potential future response to increased ocean warming could result in episodes of rapid retreat as the ice front undergoes thinning and/or ice tongue collapse. Such episodes are believed to cause a dynamic response up-glacier, resulting in an accelerated ice flow, contributing directly to sea level rise (Hill et al., 2018).

25 The lithological sequence starting with a basal till overlain by glacial marine deposits suggests the transition from sub-glacial to ice-proximal and, subsequently, to a more ice-distal environment dominated by suspension settling with various degrees of ice rafting. Evans et al. (2002) and Smith et al. (2011) documented sedimentological facies with similar characteristics from the deglaciation of the trough offshore Kejser Franz Josef Fjord and the West Antarctica Ice Sheet, respectively, implying they recorded the transition from a grounded ice sheet to open marine environments. The deglacial lithofacies (3 and 4) reflect different depositional environments (Table 2): whereas the influence from meltwater was stronger during the deposition of facies 4, the supply of IRD was higher during the deposition of facies 3. The presence of facies 4 exclusively in the two westernmost cores suggest that either the style of retreat was different between the middle and inner part of the trough, or the deglacial lithofacies deposited during the initial ice retreat was removed from the middle trough area through winnowing. However, the identification of subglacial channels in the middle part of the trough indicate that meltwater was present.

45

5.3 Postglacial development

After the deglaciation of Store Koldewey Trough, the ice stream retreated across Store Koldewey Island and Germania Land (Fig. 9: Stage 9), terminating the supply of sediment and icebergs to Store Koldewey Trough and delivering icebergs and meltwater to Dove Bugt and Jøkelbugten instead. This resulted in the termination of sediment input from this sector of the GIS to Store Koldewey Trough, which may explain the thin sediment drape on top of the glacial deposits (Fig. 7).

50



5 Postglacial sedimentary processes in the trough are interpreted to comprise hemipelagic deposition of terrestrial material in sea ice transported southwards from the Arctic Ocean with the Transpolar Drift, rainout from icebergs and meltwater plumes released from regional marine terminating outlet glaciers (e.g. 79°-Glacier and Zachariae Isstrøm), in addition to winnowing and resuspension of the finest sediment fraction within the uppermost lithological unit.

10 The low IRD content in facies 2 probably reflects a combination of ice fronts retreating from the marine realm, while icebergs from calving glaciers probably melted rapidly and only occasionally escaped the fjords. This could correlate to the Holocene Thermal Maximum (ca. 8-5 ka BP) when temperatures in NE Greenland were warmer than at present (Dahl-Jensen et al., 1998; Klug et al., 2009), causing the Storstrømmen ice margin to retreat behind its present ice-extent (Bennike and Weidick, 2001; Weidick et al., 1996). Furthermore, sea-ice formation in the Arctic Ocean and on the NE Greenland shelf was reduced during that period (Koç et al. 1993; Funder et al. 2011; Müller et al. 2012; Werner et al. 2016). The increasing input of IRD towards the top of the sediment cores (Fig. 2) is attributed to the following regional climatic cooling. The climate deterioration, referred to as the Neoglaciation (ca. 5 ka BP – Little Ice Age), lead to glacier expansion with increasing iceberg-rafting and sea-ice extent on the East Greenland shelf (Klug et al., 2009; Müller et al., 2012) (Fig. 9: Stage 9).

5.4 Possible surge activity during deglaciation

20 Crevasse-squeeze ridges are unique diagnostic landforms of glacier surges (Boulton et al., 1996; Evans and Rea, 1999; Sharp, 1985). In combination with grounding zone wedges and a seafloor characterized predominantly by iceberg ploughmarks, the landform assemblage is in coherence with the observations from Solheim (1991) in front of Bråsvellbreen, Svalbard.

25 The modern surging ice stream Storstrømmen, which presumably drained through Store Koldewey Trough under full glacial conditions during the last glacial, may have undergone similar internal disequilibrium in the past, i.e. also during the deglaciation (Fig. 9: Stage 4 and 6). If correct, this is the first study to show that also paleo-ice streams draining the GIS had a surging behavior during the deglaciation. Surge activity during ice stream retreat has been proposed for other paleo-ice streams, e.g. the Bjørnøyrenna Ice Stream (Andreassen et al., 2014) and the Irish Ice Sheet (Delaney et al., 2018), in addition to modern West-Antarctic ice streams (Bindschadler, 1997; Hughes, 1973).

35 Triggering of an active surge phase in an ice stream is suggested to be driven by internal ice dynamics constrained by both the climate and topographic environment (Sevestre and Benn, 2015). If so, a coupling between climate as a single factor and paleo-grounding line positions in regions with surging glaciers may be problematic, possibly resulting in inaccurate climate reconstructions and modelling of the response contemporary ice sheets to future climate change (e.g. the West Antarctic Ice Sheet).

40 Possible surges in Store Koldewey Trough during the deglaciation could have caused an abrupt ice front collapse and reduction in the buttressing effect, leading to an increased mass flux and a larger ice volume released into the marine environment relative to other non-surging ice streams (compare with Dupont and Alley (2005) and Royston and Gudmundsson (2016)). Thus, the ice streams draining through Store Koldewey Trough might have acted as a major agent of transferring large volumes of ice from the interior of the GIS to its margin during the early deglaciation.

45

6 Conclusions

- Mega-scale glacial lineations and a grounding zone wedge in the outer part of Store Koldewey Trough, NE Greenland, suggest that fast-flowing, grounded ice reached the continental shelf break during the LGM.



- The ice stream probably originated from the area presently covered with the Storstrømmen ice stream, cutting across Store Koldewey Island and Germania Land.
 - Multiple halts and/or readvances interrupted the deglaciation.
 - 5 • The more complex assemblage of landforms in Store Koldewey Trough relative to other ice stream settings on high-latitude continental shelves is attributed to the ice retreating into shallower water during deglaciation. Thus, the retreat/readvances in Store Koldewey Trough during deglaciation probably occurred asynchronously relative to other ice streams offshore NE Greenland.
 - Two sets of crevasse-squeezed ridges may indicate that the ice stream underwent at least two surges during the deglaciation.
 - 10 • At a late stage of the deglaciation, the ice stream retreated across Store Koldewey Island and Germania Land, terminating the sediment input from the GIS to Store Koldewey Trough.
 - Subglacial till fills the trough, with an overlying drape of postglacial sediments (<2.5 m).
- 15 *Author contributions.* The idea of the study developed from repeated discussions among the authors of this study and the opportunity to participate in a scientific cruise to the study area. ILO, JS and TAR collected the data during the *TUNU VII* cruise. The geophysical data was interpreted by ILO with help from MF, JSL and TAR. ILO conducted sample preparation and analyses of sediment data with help from KH. ILO wrote the manuscript with contributions from all authors.
- 20 *Competing interests.* The authors declare that they have no conflict of interest.



References

- Aagaard, K. and Coachman, L. K.: The East Greenland Current North of Denmark Strait : Part I, *Arctic*, 21(3), 181–200, 1968.
- Andreassen, K., Winsborrow, M. C. M., Bjarnadóttir, L. R. and Rüther, D. C.: Ice stream retreat dynamics inferred from an assemblage of landforms in the northern Barents Sea, *Quaternary Sci. Rev.*, 92, 246–257, doi:10.1016/j.quascirev.2013.09.015, 2014.
- Andrews, J. T., Cooper, T. A., Jennings, A. E., Stein, A. B. and Erlenkeuser, H.: Late quaternary iceberg-rafted detritus events on the Denmark Strait-Southeast Greenland continental slope (~65°N): Related to North Atlantic Heinrich events?, *Mar. Geol.*, 149(1–4), 211–228, doi:10.1016/S0025-3227(98)00029-2, 1998.
- Arndt, J. E.: Marine geomorphological record of Ice Sheet development in East Greenland since the Last Glacial Maximum, *J. Quaternary Sci.*, 33, 853–864, doi:10.1002/jqs.3065, 2018.
- Arndt, J. E., Jokat, W., Dorschel, B., Myklebust, R., Dowdeswell, J. A. and Evans, J.: A new bathymetry of the Northeast Greenland continental shelf: Constraints on glacial and other processes, *Geochem. Geophys. Geosy.*, doi:10.1002/2015GC005931, 2015.
- Arndt, J. E., Jokat, W. and Dorschel, B.: The last glaciation and deglaciation of the Northeast Greenland continental shelf revealed by hydro-acoustic data, *Quaternary Sci. Rev.*, 160, 45–56, doi:10.1016/j.quascirev.2017.01.018, 2017.
- Bamber, J. L., Ekholm, S. and Krabill, W. B.: A new, high-resolution digital elevation model of Greenland fully data, *J. Geophys. Res.*, 106(B4), 6733–6745, 2001.
- Bamber, J. L., Riva, R. E. M., Vermeersen, B. L. A. and Lebrocq, A. M.: Reassessment of the Potential of the West Antarctic Ice Sheet, *Science*, 324(May), 901–904, doi:10.1126/science.1169335, 2009.
- Batchelor, C. L. and Dowdeswell, J. A.: The physiography of High Arctic cross-shelf troughs, *Quaternary Sci. Rev.*, 92, 68–96, doi:10.1016/j.quascirev.2013.05.025, 2014.
- Batchelor, C. L. and Dowdeswell, J. A.: Ice-sheet grounding-zone wedges (GZWs) on high-latitude continental margins, *Mar. Geol.*, 363, 65–92, doi:10.1016/j.margeo.2015.02.001, 2015.
- Bendtsen, J., Mortensen, J., Lennert, K., Ehn, J. K., Boone, W., Galindo, V., Hu, Y. Bin, Dmitrenko, I. A., Kirillov, S. A., Kjeldsen, K. K., Kristoffersen, Y., Barber, D. G. and Rysgaard, S.: Sea ice breakup and marine melt of a retreating tidewater outlet glacier in northeast Greenland (81°N), *Sci. Rep-UK*, 7(1), 1–11, doi:10.1038/s41598-017-05089-3, 2017.
- Bennike, O. and Weidick, A.: Late Quaternary history around Nioghalvfjærdsfjorden and Jøkelbugten, North-East Greenland, *Boreas*, 30(3), 205–227, doi:DOI: 10.1111/j.1502-3885.2001.tb01223.x, 2001.
- Bennike, O., Björck, S. and Lambeck, K.: Estimates of South Greenland late-glacial ice limits from a new relative sea level curve, *Earth. Planet. Sc. Lett.*, 197(3–4), 171–186, doi:10.1016/S0012-821X(02)00478-8, 2002.
- Bentley, C. R.: Antarctic ice streams: a review, *J. Geophys. Res.*, 92(6), 8843–8858, 1987.
- Bindschadler, R.: Actively surging West Antarctic ice streams and their response characteristics, *Ann. Glaciol.*, 24, 409–414, 1997.
- Bjarnadóttir, L. R., Rüther, D. C., Winsborrow, M. C. M. and Andreassen, K.: Grounding-line dynamics during the last deglaciation of Kveithola, W Barents Sea, as revealed by seabed geomorphology and shallow seismic stratigraphy, *Boreas*, 42(1), 84–107, doi:10.1111/j.1502-3885.2012.00273.x, 2013.
- Blott, S. J. and Pye, K.: GRADISTAT: a grain size distribution and statistics package for the analysis of unconsolidated sediments, *Earth. Surf. Proc. Land.*, 26, 1237–1248, doi:10.1016/S0167-5648(08)70015-7, 2001.
- Boulton, G. S.: Sedimentary and sea level changes during glacial cycles and their control on glacial marine facies architecture., in *Glacial marine environments: Processes and Sediments*, edited by J. A. Dowdeswell and J. D. Scourse, pp. 15–52, Geological Society Special Publications., 1990.
- Boulton, G. S. and Deynoux, M.: Sedimentation in glacial environments and the identification of tills and tillites



- in ancient sedimentary sequences, *Precambrian Res.*, 15(3–4), 397–422, doi:10.1016/0301-9268(81)90059-0, 1981.
- 5 Boulton, G. S., van der Meer, J. J. M., Hart, J., Beets, D., Ruegg, G. H. J., Wateren, van der, F. M. and Jarvis, J.: Till and moraine emplacement in a deforming bed surge - an example from a marine environment, *Quaternary Sci. Rev.*, 15(95), 961–987, 1996.
- Boulton, G. S., Hagdorn, M. and Hulton, N. R. J.: Streaming flow in an ice sheet through a glacial cycle, *Ann. Glaciol.*, 36(1985), 117–128, doi:10.3189/172756403781816293, 2003.
- Canals, M., Urgeles, R. and Calafat, A. M.: Deep sea-floor evidence of past ice streams off the Antarctic Peninsula, *Geology*, 28(1), 31–34, doi:10.1130/0091-7613(2000)028<0031:DSEOPI>2.0.CO;2, 2000.
- 10 Christiansen, J. S.: The TUNU-programme: euro-arctic marine fishes – diversity and adaption., in *Adaptation and Evolution in Marine Environments, Volume 1. From Pole to Pole.*, edited by V. C. Di Prisco G, pp. 35–50, Springer, Berlin, Heidelberg., 2012.
- Clark, C. D.: Mega-scale glacial lineations and cross-cutting ice-flow landforms, *Earth. Surf. Proc. Land.*, 18, 1–29, 1993.
- 15 Cofaigh, C. Ó., Evans, D. J. A. and Smith, I. R.: Large-scale reorganization and sedimentation of terrestrial ice streams during late Wisconsinan Laurentide Ice Sheet deglaciation, *Bull. Geol. Soc. Am.*, 122(5–6), 743–756, doi:10.1130/B26476.1, 2010.
- Dahl-Jensen, D., Mosegaard, K., Gundestrup, N., Clow, G. D., Johnsen, S. J., Hansen, A. W. and Balling, N.: Past Temperatures Directly from the Greenland Ice Sheet, *Science*, 282, 268–271, doi:10.1126/science.282.5387.268, 1998.
- 20 Dahl-Jensen, D., Bamber, J. L., Bøggild, C. E., Buch, E., Christensen, J. H., Dethloff, K., Fahnestock, M., Marshall, S., Rosing, M., Steffen, K., Thomas, R., Truffer, M., van den Broeke, M. R. and van der Veen, C. J.: Summary: The Greenland Ice Sheet in a Changing Climate, SWIPA Snow, Water, Ice Permafrost in the Arctic (SWIPA), 1–22, doi:10.1007/s00018-010-0512-6, 2009.
- 25 Delaney, C. A., McCarron, S. and Davis, S.: Irish Ice Sheet dynamics during deglaciation of the central Irish Midlands: Evidence of ice streaming and surging from airborne LiDAR, *Geomorphology*, 306, 235–253, doi:10.1016/j.geomorph.2018.01.011, 2018.
- Dowdeswell, J. A. and Fugelli, E. M. G.: The seismic architecture and geometry of grounding-zone wedges formed at the marine margins of past ice sheets, *Geol. Soc. Am. Bull.*, 124(11–12), 1750–1761, doi:10.1130/B30628.1, 2012.
- 30 Dowdeswell, J. A. and Ottesen, D.: Submarine landform assemblage for Svalbard surge-type tidewater glaciers, *Geo. Soc. Mem.*, 46(1), 151 LP – 154, doi:10.1144/M46.160, 2016.
- Dowdeswell, J. A., Hamilton, G. S. and Hagen, J. O.: The duration of the active phase on surge-type glaciers: contrasts between Svalbard and other regions, *J. Glaciol.*, 37(127), 388–400, 1991.
- 35 Dowdeswell, J. A., Uenzelmann-Neben, G., Whittington, R. J. and Marienfeld, P.: The Late Quaternary sedimentary record in Scoresby Sund, East Greenland, *Boreas*, 23(4), 294–310, doi:10.1111/j.1502-3885.1994.tb00602.x, 1994.
- Dowdeswell, J. A., Ottesen, D., Evans, J., Cofaigh, C. Ó. and Anderson, J. B.: Submarine glacial landforms and rates of ice-stream collapse, *Geology*, doi:10.1130/G24808A.1, 2008.
- 40 Dupont, T. K. and Alley, R. B.: Assessment of the importance of ice-shelf buttressing to ice-sheet flow, *Geophys. Res. Lett.*, 32(4), 1–4, doi:10.1029/2004GL020224, 2005.
- Evans, D. J. A. and Rea, B. R.: Geomorphology and sedimentology of surging glaciers: a land-systems approach, *Ann. Glaciol.*, 28, 75–82, 1999.
- 45 Evans, D. J. A., Phillips, E. R., Hiemstra, J. F. and Auton, C. A.: Subglacial till: Formation, sedimentary characteristics and classification, *Earth-Sci. Rev.*, 78(1–2), 115–176, doi:10.1016/j.earscirev.2006.04.001, 2006.
- Evans, J., Dowdeswell, J. A., Grobe, H., Niessen, F., Stein, R., Hubberten, H.-W. and Whittington, R. J.: Late Quaternary sedimentation in Kejsers Franz Joseph Fjord and the continental margin of East Greenland, *Geol. Soc. Spec. Publ.*, 203(1), 149–179, doi:10.1144/GSL.SP.2002.203.01.09, 2002.



- Evans, J., Ó Cofaigh, C., Dowdeswell, J. A. and Wadhams, P.: Marine geophysical evidence for former expansion and flow of the Greenland Ice Sheet across the north-east Greenland continental shelf, *J. Quaternary Sci.*, doi:10.1002/jqs.1231, 2009.
- 5 Fahnestock, M., Bindschadler, R., Kwok, R. and Jezek, K.: Greenland Ice Sheet surface properties and ice dynamics from ERS-1 SAR imagery, *Science*, 262(5139), 1530–1534, doi:10.1126/science.262.5139.1530, 1993.
- Funder, S., Goosse, H., Jepsen, H., Kaas, E., Kjær, K. H., Korsgaard, N. J., Larsen, N. K., Linderson, H., Lyså, A., Möller, P., Olsen, J. and Willerslev, E.: A 10,000-Year Record of Arctic Ocean Sea-Ice Variability—View from the Beach, *Science*, 333, 747–750, doi:10.2307/j.ctv9zcyj2n.53, 2011a.
- 10 Funder, S., Kjeldsen, K. K., Kjær, K. H. and Ó Cofaigh, C.: The Greenland Ice Sheet During the Past 300,000 Years: A Review, *Developments in Quaternary Sciences*, 15(December), 699–713, doi:10.1016/B978-0-444-53447-7.00050-7, 2011b.
- Fürst, J. J., Goelzer, H. and Huybrechts, P.: Ice-dynamic projections of the Greenland ice sheet in response to atmospheric and oceanic warming, *The Cryosphere*, 9(3), 1039–1062, doi:10.5194/tc-9-1039-2015, 2015.
- 15 Hansbo, S.: A new approach to the determination of the shear strength of clay by the fall-cone test, *Royal Swedish Geotechnical Institute.*, 1957.
- Henriksen, N. and Higgins, A. K.: Descriptive text to the Geological map of Greenland , 1 : 500 000 , Dove Bugt , Sheet 10, GEUS., 2009.
- Hill, E. A., Carr, J. R., Stokes, C. R. and Gudmundsson, G. H.: Dynamic changes in outlet glaciers in northern Greenland from 1948 to 2015, *The Cryosphere*, 1–39, doi:10.5194/tc-2018-17, 2018.
- 20 Hogan, K. A., Dix, J. K., Lloyd, J. M., Long, A. J. and Cotterill, C. J.: Seismic stratigraphy records the deglacial history of Jakobshavn Isbræ, West Greenland, *J. Quaternary Sci.*, 26(7), 757–766, doi:10.1002/jqs.1500, 2011.
- Hogan, K. A., Colm, O., Jennings, A. E., Dowdeswell, J. A. and Hiemstra, J. F.: Deglaciation of a major palaeo-ice stream in Disko Trough , West Greenland, *Quaternary Sci. Rev.*, 147, 5–26, doi:10.1016/j.quascirev.2016.01.018, 2016.
- 25 Hopkins, T. S.: The GIN Sea-A synthesis of its physical oceanography and literature review 1972-1985, *Earth-Sci. Rev.*, 30(3–4), 175–318, doi:10.1016/0012-8252(91)90001-V, 1991.
- Hubberten, H., Grobe, H., Jokat, W., Melles, M., Niessen, F. and Stein, R.: Glacial history of East Greenland explored, *Eos Trans. AGU*, 76(36), 353–356, 1995.
- Hughes, T.: Is the West Antarctic Ice Sheet, *J. Geophys. Res.*, 78(33), 7884–7910, 1973.
- 30 IPCC: IPCC special report on the impacts of global warming of 1.5 °C - Summary for policy makers, , (October 2018) [online] Available from: <http://www.ipcc.ch/report/sr15/>, 2018.
- Jakobsson, M., Anderson, J. B., Nitsche, F. O., Gyllencreutz, R., Kirshner, A. E., Kirchner, N., O'Regan, M., Mohammad, R. and Eriksson, B.: Ice sheet retreat dynamics inferred from glacial morphology of the central Pine Island Bay Trough, West Antarctica, *Quaternary Sci. Rev.*, 38, 1–10, doi:10.1016/j.quascirev.2011.12.017, 2012a.
- 35 Jakobsson, M., Mayer, L., Coakley, B., Dowdeswell, J. A., Forbes, S., Fridman, B., Hodnesdal, H., Noormets, R., Pedersen, R., Rebesco, M., Schenke, H. W., Zarayskaya, Y., Accettella, D., Armstrong, A., Anderson, R. M., Bienhoff, P., Camerlenghi, A., Church, I., Edwards, M., Gardner, J. V., Hall, J. K., Hell, B., Hestvik, O., Kristoffersen, Y., Marcussen, C., Mohammad, R., Mosher, D., Nghiem, S. V., Pedrosa, M. T., Travaglini, P. G. and Weatherall, P.: The International Bathymetric Chart of the Arctic Ocean (IBCAO) Version 3.0, *Geophys. Res. Lett.*, 39(12), 1–6, doi:10.1029/2012GL052219, 2012b.
- 40 Jennings, A. E. and Weiner, N. J.: Environmental change in eastern Greenland during the last 1300 years : evidence from foraminifera and lithofacies in Nansen Fjord, 68°N, *The Holocene*, 6(2), 179–191, 1996.
- Jennings, A. E., Reilly, B., Andrews, J. T., Hogan, K. A., Walczak, M., Stoner, J., Mix, A. and Jakobsson, M.: Sedimentological and faunal evidence of ice shelves during the Early Holocene deglaciation of Nares Strait, in 49th International Arctic Workshop, Program and Abstracts 2019, p. 67, Stockholm University., 2019.
- 45 Joughin, I. R., Fahnestock, M. A. and Bamber, J. L.: Ice flow in the northeast Greenland ice stream, *Ann. Glaciol.*, 31, 141–146, doi:10.1016/j.radphyschem.2012.12.021, 2000.



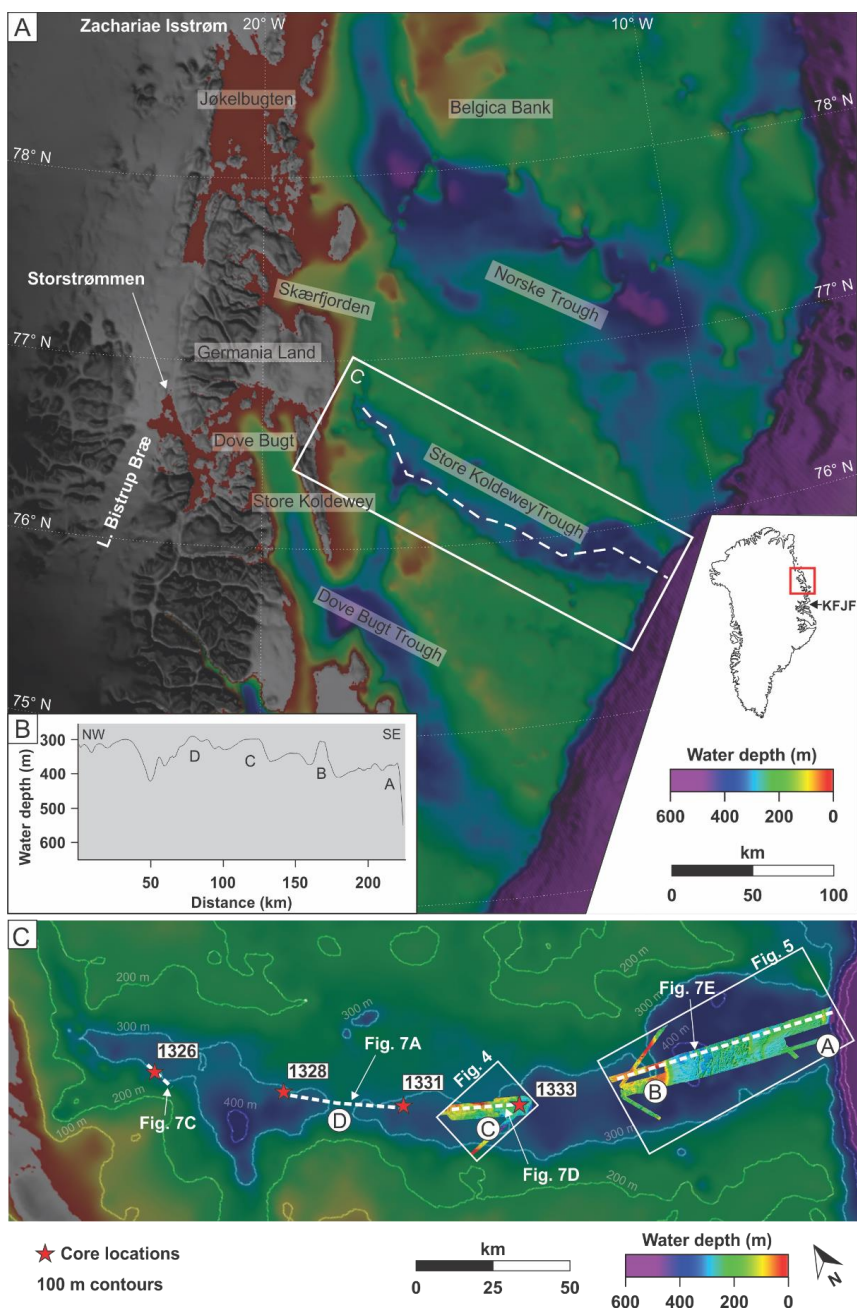
- Khan, S. A., Kjær, K. H., Bevis, M., Bamber, J. L., Wahr, J., Kjeldsen, K. K., Bjørk, A. A., Korsgaard, N. J., Stearns, L. A., Van Den Broeke, M. R., Liu, L., Larsen, N. K. and Muresan, I. S.: Sustained mass loss of the northeast Greenland ice sheet triggered by regional warming, *Nat. Clim. Change*, 4(4), 292–299, doi:10.1038/nclimate2161, 2014.
- 5 King, E. C., Hindmarsh, R. C. A. and Stokes, C. R.: Formation of mega-scale glacial lineations observed beneath a West Antarctic ice stream, *Nat. Geosci.*, 2(8), 585–588, doi:10.1038/ngeo581, 2009.
- Klages, J. P., Kuhn, G., Hillenbrand, C. D., Graham, A. G. C., Smith, J. A., Larter, R. D. and Gohl, K.: First geomorphological record and glacial history of an inter-ice stream ridge on the West Antarctic continental shelf, *Quaternary Sci. Rev.*, 61, 47–61, doi:10.1016/j.quascirev.2012.11.007, 2013.
- 10 Klug, M., Bennike, O. and Wagner, B.: Repeated short-term bioproductivity changes in a coastal lake on Store Koldewey, northeast Greenland: An indicator of varying sea-ice coverage?, *The Holocene*, 19(4), 653–663, doi:10.1177/0959683609104040, 2009.
- Koç, N., Jansen, E. and Haflidason, H.: Paleoceanographic reconstructions of surface ocean conditions in the Greenland, Iceland and Norwegian Seas through the last 14 ka based on diatoms, *Quaternary Sci. Rev.*, 12, 115–140, 1993.
- 15 Koch, I. P.: Survey of Northeast Greenland (Danmark Expedition 1906-08), *Meddelelser om Grønland.*, 46(2), 79–468, 1916.
- Kristoffersen, Y., Coakley, B., Jokat, W., Edwards, M., Brekke, H. and Gjengedal, J.: Seabed erosion on the Lomonosov Ridge, central Arctic Ocean: A tale of deep draft icebergs in the Eurasia Basin and the influence of Atlantic water inflow on iceberg motion?, *Paleoceanography*, 19(3), 1–14, doi:10.1029/2003PA000985, 2004.
- 20 Laberg, J. S., Forwick, M. and Husum, K.: New geophysical evidence for a revised maximum position of part of the NE sector of the Greenland ice sheet during the last glacial maximum, *Arktos*, 3(1), 3, doi:10.1007/s41063-017-0029-4, 2017.
- Lambeck, K., Rouby, H., Purcell, A., Sun, Y. and Sambridge, M.: Sea level and global ice volumes from the Last Glacial Maximum to the Holocene, *P. Natl. Acad. Sci. USA*, 111(43), 15296–15303, doi:10.1073/pnas.1411762111, 2014.
- 25 Landvik, J. Y.: The last glaciation of Germania Land and adjacent areas, northeast Greenland, *J. Quaternary Sci.*, 9(1), 81–92, doi:10.1002/jqs.3390090108, 1994.
- Lenton, T. M., Held, H., Kriegler, E., Hall, J. W., Lucht, W., Rahmstorf, S. and Joachim, H.: Tipping elements in the Earth’s climate system, *P. Natl. Acad. Sci. USA*, 105(6), 1786–1793, doi:10.1073/pnas.0705414105, 2008.
- 30 Mayer, C., Schaffer, J., Hattermann, T., Floricioiu, D., Krieger, L., Dodd, P. A., Kanzow, T., Licciulli, C. and Schannwell, C.: Large ice loss variability at Nioghalvfjærdsfjorden Glacier, Northeast-Greenland, *Nat. Commun.*, 9(1), 1–11, doi:10.1038/s41467-018-05180-x, 2018.
- 35 Moon, T., Joughin, I. and Smith, B.: Seasonal to multiyear variability of glacier surface velocity, terminus position, and sea ice/ice mélange in northwest Greenland, *J. Geophys. Res.-Earth*, 120, 818–833, doi:10.1002/2015JF003494, 2015.
- Mouginot, J., Bjørk, A. A., Millan, R., Scheuchl, B. and Rignot, E.: Insights on the surge behavior of Storstrømmen and L. Bistrup Bræ, northeast Greenland, over the last century., *Geophys. Res. Lett.*, 45, 11,197-11,205, doi:10.1029/2018GL079052, 2018.
- 40 Mulder, T., Syvitski, J. P. M., Migeon, S., Faugères, J. C. and Savoye, B.: Marine hyperpycnal flows: Initiation, behavior and related deposits. A review, *Mar. Petrol. Geol.*, 20(6–8), 861–882, doi:10.1016/j.marpetgeo.2003.01.003, 2003.
- Müller, J., Werner, K., Stein, R., Fahl, K., Moros, M. and Jansen, E.: Holocene cooling culminates in sea ice oscillations in Fram Strait, *Quaternary Sci. Rev.*, 47, 1–14, doi:10.1016/j.quascirev.2012.04.024, 2012.
- 45 Munsell, A. H.: Munsell soil color charts, Munsell Color Company, doi:10.1111/1911-3846.12037, 2000.
- Nick, F. M., Vieli, A., Andersen, M. L., Joughin, I., Payne, A., Edwards, T. L., Pattyn, F. and Van De Wal, R. S. W.: Future sea-level rise from Greenland’s main outlet glaciers in a warming climate, *Nature*, 497(7448), 235–238, doi:10.1038/nature12068, 2013.



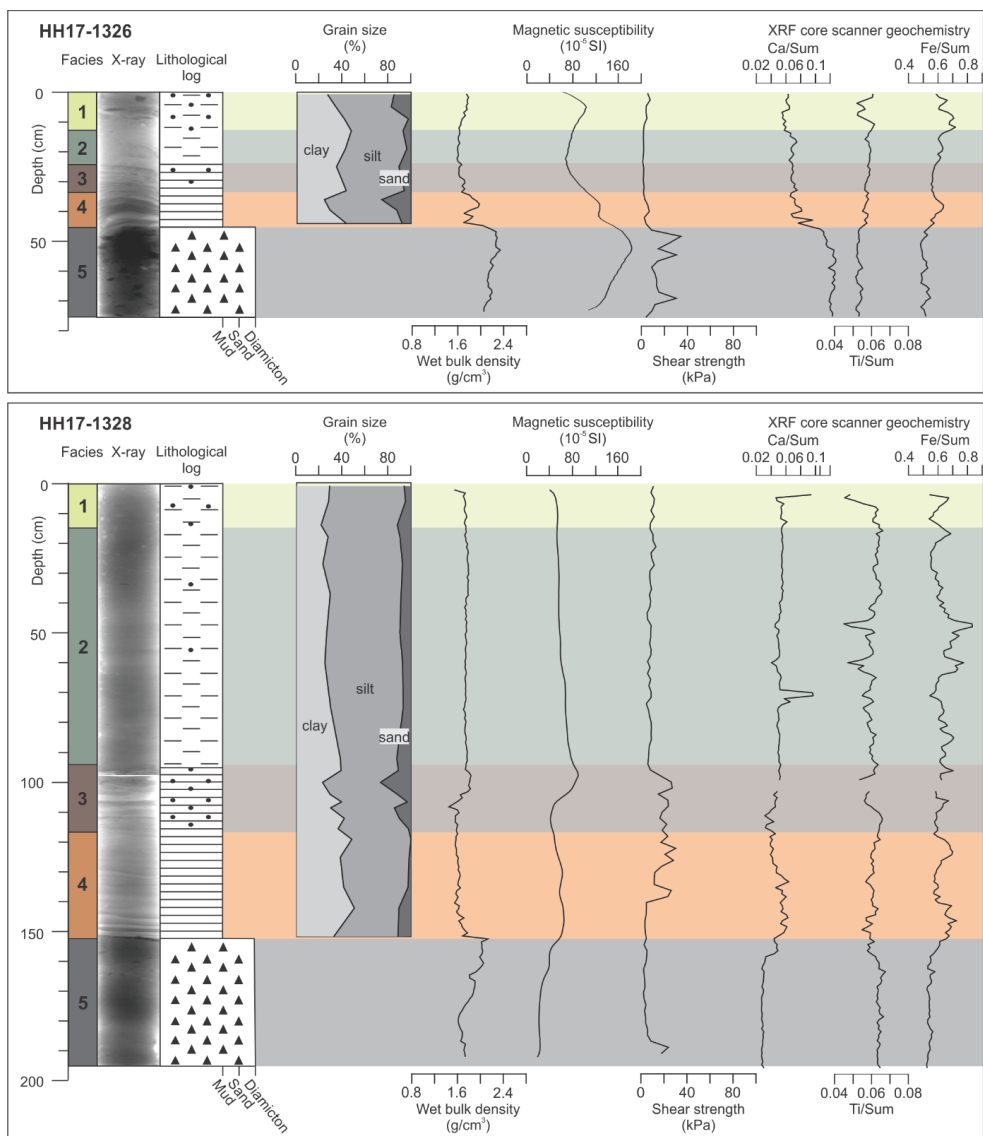
- Ó Cofaigh, C. and Dowdeswell, J. A.: Laminated sediments in glacial marine environments: Diagnostic criteria for their interpretation, *Quaternary Sci. Rev.*, 20(13), 1411–1436, doi:10.1016/S0277-3791(00)00177-3, 2001.
- 5 Ó Cofaigh, C., Dowdeswell, J. A., Evans, J., Kenyon, N. H., Taylor, J., Mienert, J. and Wilken, M.: Timing and significance of glacially influenced mass-wasting in the submarine channels of the Greenland Basin, *Mar. Geol.*, 207(1–4), 39–54, doi:10.1016/j.margeo.2004.02.009, 2004.
- Ó Cofaigh, C., Evans, J., Dowdeswell, J. A. and Larter, R. D.: Till characteristics, genesis and transport beneath Antarctic paleo-ice streams, *J. Geophys. Res.-Earth*, 112(3), 1–16, doi:10.1029/2006JF000606, 2007.
- Ó Cofaigh, C., Dowdeswell, J. A., Evans, J. and Larter, R. D.: Geological constraints on Antarctic palaeo-ice-stream retreat, *Earth. Surf. Proc. Land.*, 33, 513–525, doi:10.1002/esp, 2008.
- 10 Ó Cofaigh, C., Dowdeswell, J. A., Jennings, A. E., Hogan, K. A., Kilfeather, A., Hiemstra, J. F., Noormets, R., Evans, J., McCarthy, D. J., Andrews, J. T., Lloyd, J. M. and Moros, M.: An extensive and dynamic ice sheet on the west Greenland shelf during the last glacial cycle, *Geology*, 41(2), 219–222, doi:10.1130/G33759.1, 2013.
- Ottesen, D. and Dowdeswell, J. A.: An inter-ice-stream glaciated margin: Submarine landforms and a geomorphic model based on marine-geophysical data from Svalbard, *Bull. Geol. Soc. Am.*, 121(11–12), 1647–1665, doi:10.1130/B26467.1, 2009.
- 15 Ottesen, D., Dowdeswell, J. A. and Rise, L.: Submarine landforms and the reconstruction of fast-flowing ice streams within a large Quaternary ice sheet: The 2500-km-long Norwegian-Svalbard margin (57°–80°N), *Bull. Geol. Soc. Am.*, 117(7–8), 1033–1050, doi:10.1130/B25577.1, 2005.
- Rignot, E. and Kanagaratnam, P.: Changes in the velocity structure of the Greenland Ice Sheet, *Science*, 311(5763), 986–990, doi:10.1126/science.1121381, 2006.
- 20 Royston, S. and Gudmundsson, G. H.: Changes in ice-shelf buttressing following the collapse of Larsen A Ice Shelf, Antarctica, and the resulting impact on tributaries, *J. Glaciol.*, 62(235), 905–911, doi:10.1017/jog.2016.77, 2016.
- Rydningen, T. A., Vorren, T. O., Laberg, J. S. and Kolstad, V.: The marine-based NW Fennoscandian ice sheet: Glacial and deglacial dynamics as reconstructed from submarine landforms, *Quaternary Sci. Rev.*, 68, 126–141, doi:10.1016/j.quascirev.2013.02.013, 2013.
- 25 Serreze, M. C. and Francis, J. A.: The arctic amplification debate, *Climatic Change*, 76(3–4), 241–264, doi:10.1007/s10584-005-9017-y, 2006.
- Sevestre, H. and Benn, D. I.: Climatic and geometric controls on the global distribution of surge-type glaciers: Implications for a unifying model of surging, *J. Glaciol.*, 61(228), 646–662, doi:10.3189/2015JG14J136, 2015.
- 30 Sharp, M.: “Crevasse-Fill” Ridges—A Landform Type Characteristic of Surging Glaciers?, *Geogr. Ann. A.*, 67(3–4), 213–220, doi:10.1080/04353676.1985.11880147, 1985.
- Smith, J. A., Hillenbrand, C. D., Kuhn, G., Larter, R. D., Graham, A. G. C., Ehrmann, W., Moreton, S. G. and Forwick, M.: Deglacial history of the West Antarctic Ice Sheet in the western Amundsen Sea Embayment, *Quaternary Sci. Rev.*, 30(5–6), 488–505, doi:10.1016/j.quascirev.2010.11.020, 2011.
- 35 Solheim, A.: The depositional environment of surging sub-polar tidewater glaciers: a case study of the morphology, sedimentation and sediment properties in a surge affected marine basin outside Nordaustlandet, the Northern Barents Sea., *Norsk Polarinst. Skri.*, 194, 97, 1991.
- Spagnolo, M., Clark, C. D., Ely, J. C., Stokes, C. R., Anderson, J. B., Andreassen, K., Graham, A. G. C. and King, E. C.: Size, shape and spatial arrangement of mega-scale glacial lineations from a large and diverse dataset, *Earth. Surf. Proc. Land.*, 39, 1432–1448, doi:10.1002/esp.3532, 2014.
- 40 Stein, R., Nam, S.-I., Grobe, H. and Hubberten, H.-W.: Late Quaternary glacial history and short-term ice-rafted debris fluctuations along the East Greenland continental margin, in *Late Quaternary Palaeoceanography of the North Atlantic Margins*, vol. 111, edited by J. T. Andrews, W. E. N. Austin, H. Bergsten, and A. E. Jennings, pp. 135–151, Geological Society Special Publications., 1996.
- 45 Stewart, F. S. and Stoker, M. S.: Problems associated with seismic facies analysis of diamicton-dominated, shelf glacial sequences, *Geo-Mar. Lett.*, 10(3), 151–156, doi:10.1007/BF02085930, 1990.
- Stokes, C. R. and Clark, C. D.: Geomorphological criteria for identifying Pleistocene ice streams, *Ann. Glaciol.*,



- 28(4), 67–74, doi:10.3189/172756499781821625, 1999.
- Straneo, F. and Heimbach, P.: North Atlantic warming and the retreat of Greenland's outlet glaciers, *Nature*, 504(7478), 36–43, doi:10.1038/nature12854, 2013.
- 5 Vorren, T. O. and Plassen, L.: Late weichselian and holocene sediment flux and sedimentation rates in Andfjord and Vågsfjord, North Norway, *J. Quaternary Sci.*, doi:10.1002/jqs.662, 2002.
- Vorren, T. O., Hald, M. and Lebesbye, E.: Late Cenozoic environments in the Barents Sea, *Paleoceanography*, 3(5), 601–612, 1988.
- Weber, M. E., Niessen, F., Kuhn, G. and Wiedicke, M.: Calibration and application of marine sedimentary physical properties using a multi-sensor core logger, *Mar. Geol.*, 136(3–4), 151–172, 1997.
- 10 Weidick, A., Andreasen, C., Oerter, H. and Reeh, N.: Neoglacial glacier changes around Storstrommen, north-east Greenland, *Polarforschung*, 64(3), 95–108, 1996.
- Werner, K., Müller, J., Husum, K., Spielhagen, R. F., Kandiano, E. S. and Polyak, L.: Holocene sea subsurface and surface water masses in the Fram Strait – Comparisons of temperature and sea-ice reconstructions, *Quaternary Sci. Rev.*, 147, 194–209, doi:10.1016/j.quascirev.2015.09.007, 2016.
- 15 Wilson, N. J. and Straneo, F.: Water exchange between the continental shelf and the cavity beneath Nioghalvfjærdsbræ (79 North Glacier), *Geophys. Res. Lett.*, 42(18), 7648–7654, doi:10.1002/2015GL064944, 2015.
- Winkelmann, D., Jokat, W., Jensen, L. and Schenke, H. W.: Submarine end moraines on the continental shelf off NE Greenland - Implications for Lateglacial dynamics, *Quaternary Sci. Rev.*, 29(9–10), 1069–1077, doi:10.1016/j.quascirev.2010.02.002, 2010.
- 20 Winsborrow, M. C. M., Andreassen, K., Corner, G. D. and Laberg, J. S.: Deglaciation of a marine-based ice sheet: Late Weichselian palaeo-ice dynamics and retreat in the southern Barents Sea reconstructed from onshore and offshore glacial geomorphology, *Quaternary Sci. Rev.*, 29(3–4), 424–442, doi:10.1016/j.quascirev.2009.10.001, 2010.
- 25 Wise, M. G., Dowdeswell, J. A., Jakobsson, M. and Larter, R. D.: Evidence of marine ice-cliff instability in Pine Island Bay from iceberg-keel plough marks, *Nature*, 550(7677), 506–510, doi:10.1038/nature24458, 2017.



5 **Figure 1:** (A) Overview of the regional bathymetry and the hinterland topography of northeast Greenland (from IBCAO v.3.0; Jakobsson et al. 2012b) including geographical names. The small map show Greenland and the location of Kejser Franz Josef Fjord (KFJF). White dashed line shows the location of bathymetric profile shown in (B). (B) Bathymetric profile of Store Koldewey Trough. The labels A-D show the locations of interpreted grounding-zone wedges as described by Laberg et al. (2017). (C) Large-scale bathymetry of Store Koldewey Trough (from IBCAO v.3.0; Jakobsson et al. 2012b) including the swath bathymetry data analyzed in this study. The labels A-D represent grounding-zone wedges (adapted from Laberg et al. 2017), red stars show core locations.



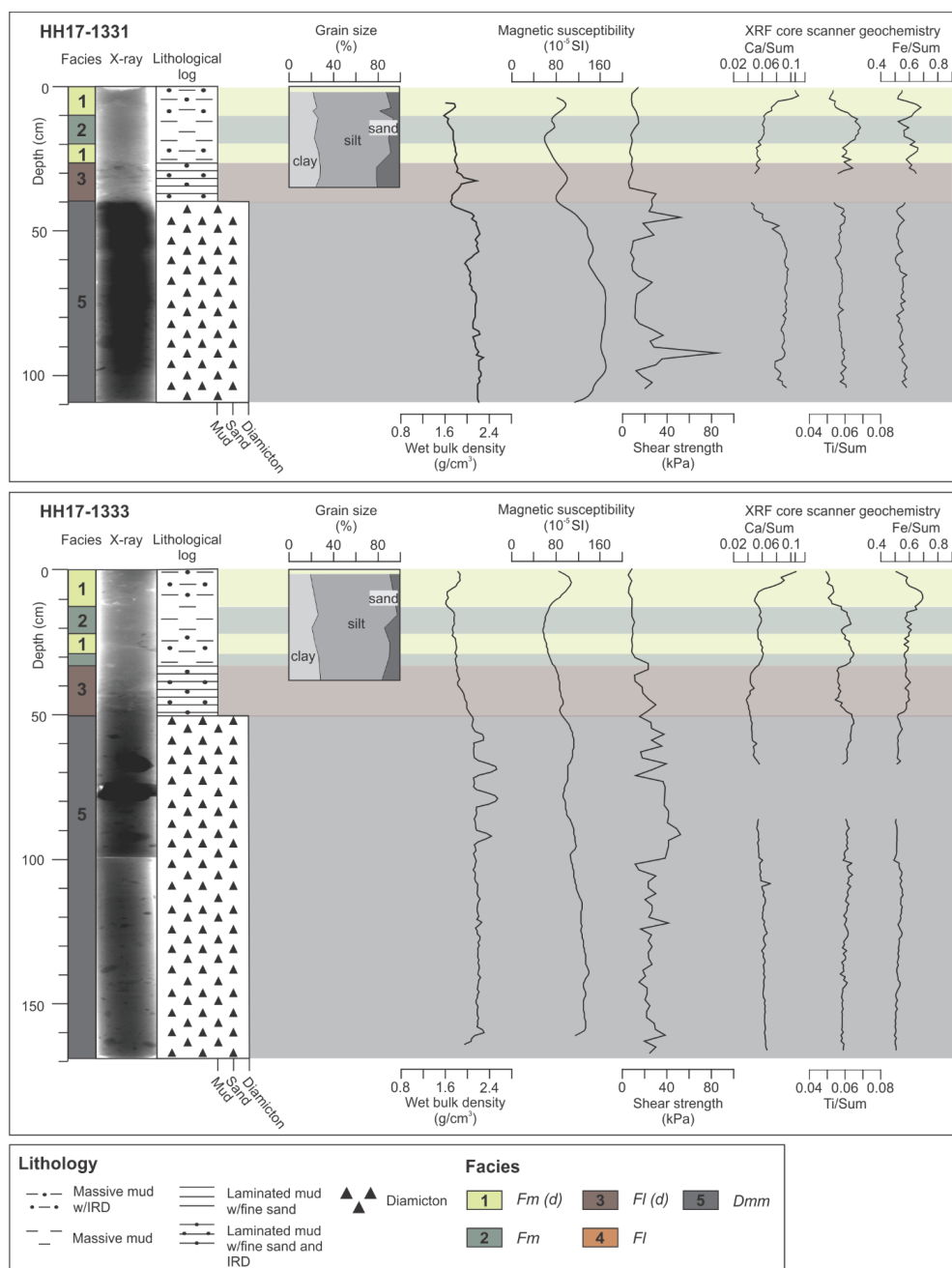


Figure 2. Sedimentary lithofacies logs, X-radiographs, grain-size distribution, physical properties and XRF core scanning geochemistry for the cores from inner and middle Store Koldewey Trough. The darker grey tones in the X-radiographs reflect higher density, whereas brighter grey tones reflect lower density. The locations of the sediment cores are shown in Fig. 1C.

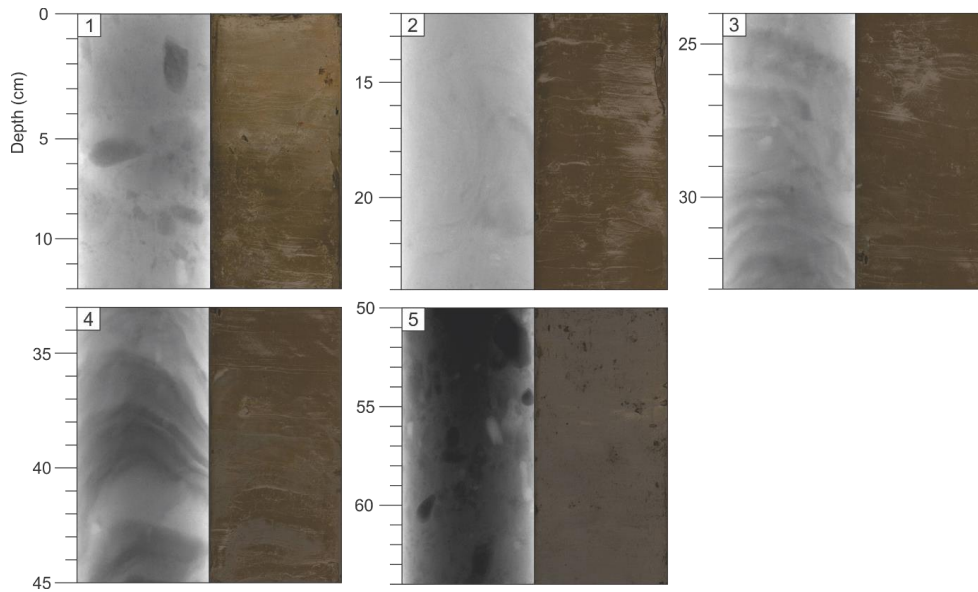


Figure 3. X-radiographs with associated photographs of representative lithofacies in this study, all from core HH17-1326. (1) Massive mud with IRD (Fm (d)). (2) Massive mud (Fm). (3) Laminated mud with occasional IRD (Fl (d)). (4) Laminated mud (Fl). (5) Diamicton (Dmm). The darker grey tones on the X-radiographs reflect higher density, whereas brighter grey tones reflect lower density.

5

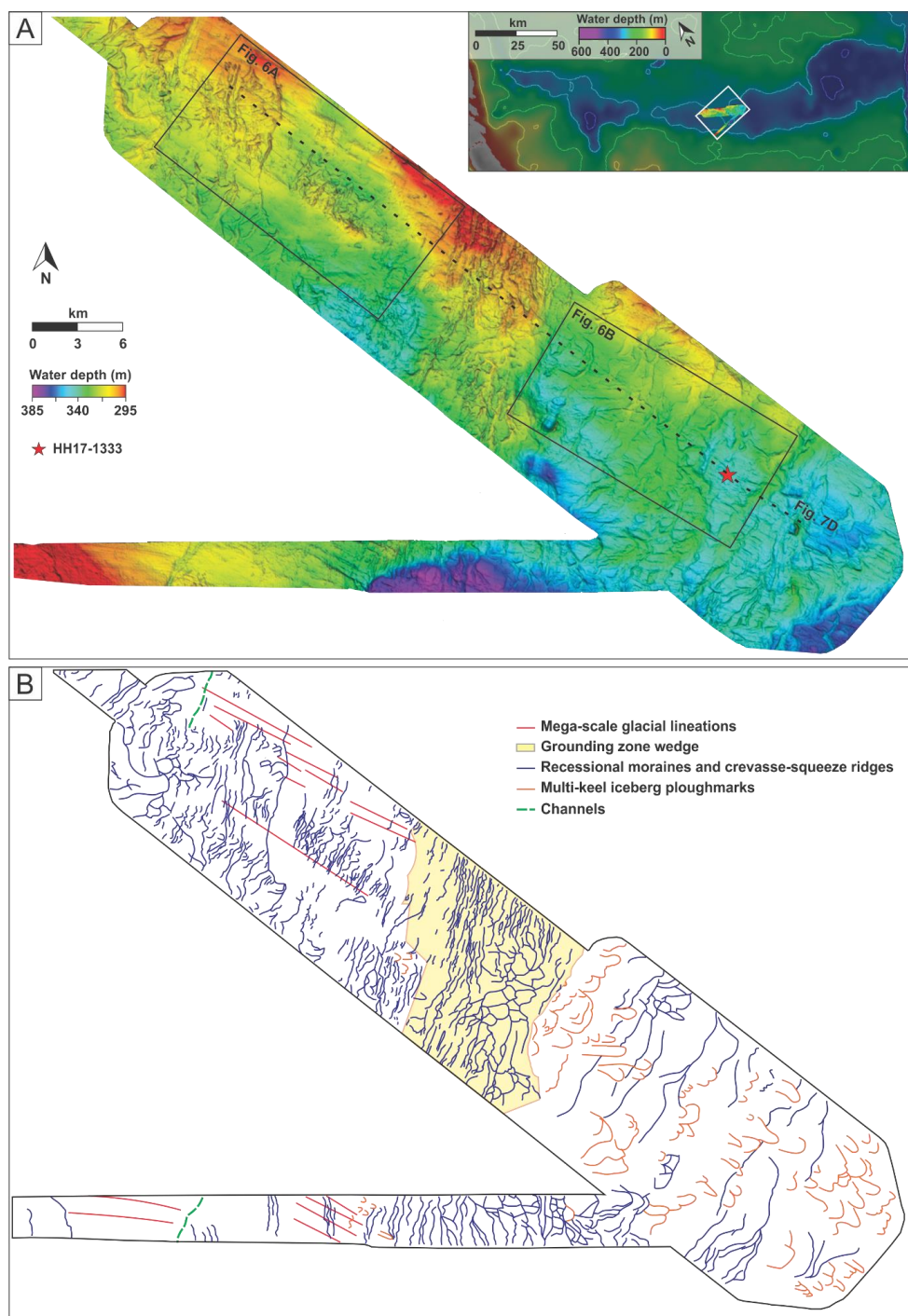


Figure 4. (A) Swath bathymetry map from the middle part of Store Koldewey Trough. (B) Distribution of mapped landforms.

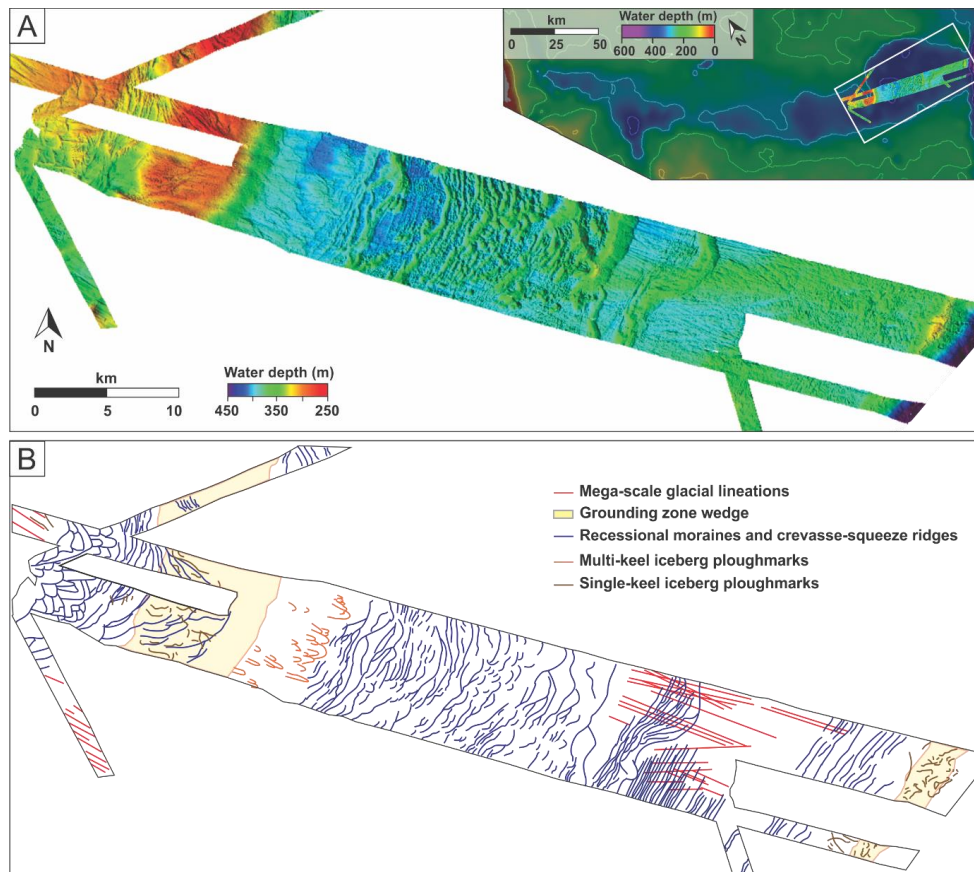


Figure 5. (A) Swath bathymetry map from the outer part of Store Koldewey Trough. (B) Interpretation and distribution of landforms.

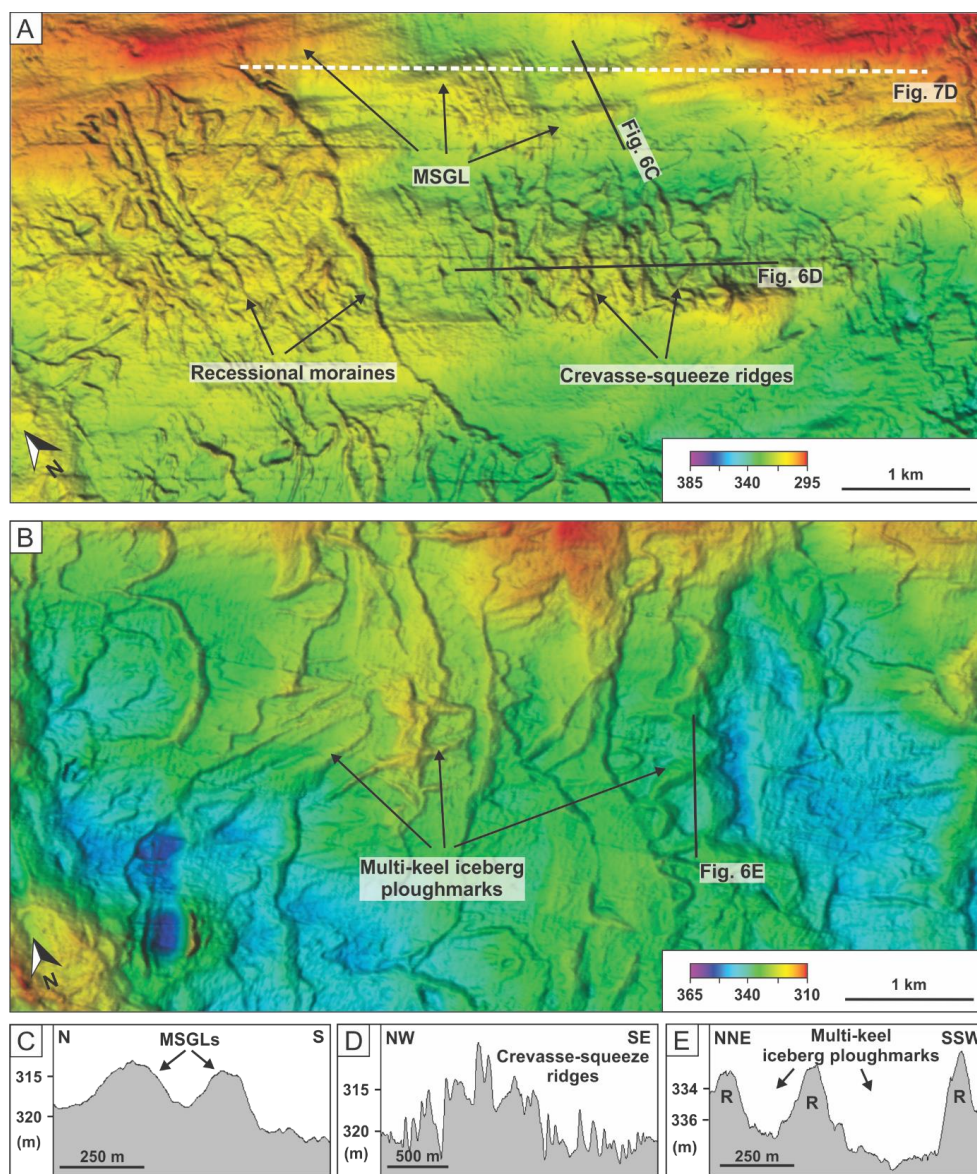


Figure 6. (A) Examples of MSGLs, recessional moraines and crevasse-squeeze ridges. (B) Examples of multi-keel iceberg ploughmarks. (C) Bathymetric cross-profile of MSGLs. (D) Bathymetric cross-profile of crevasse-squeeze ridges. (E) Bathymetric profile of multi-keel iceberg ploughmarks. R= ridges.

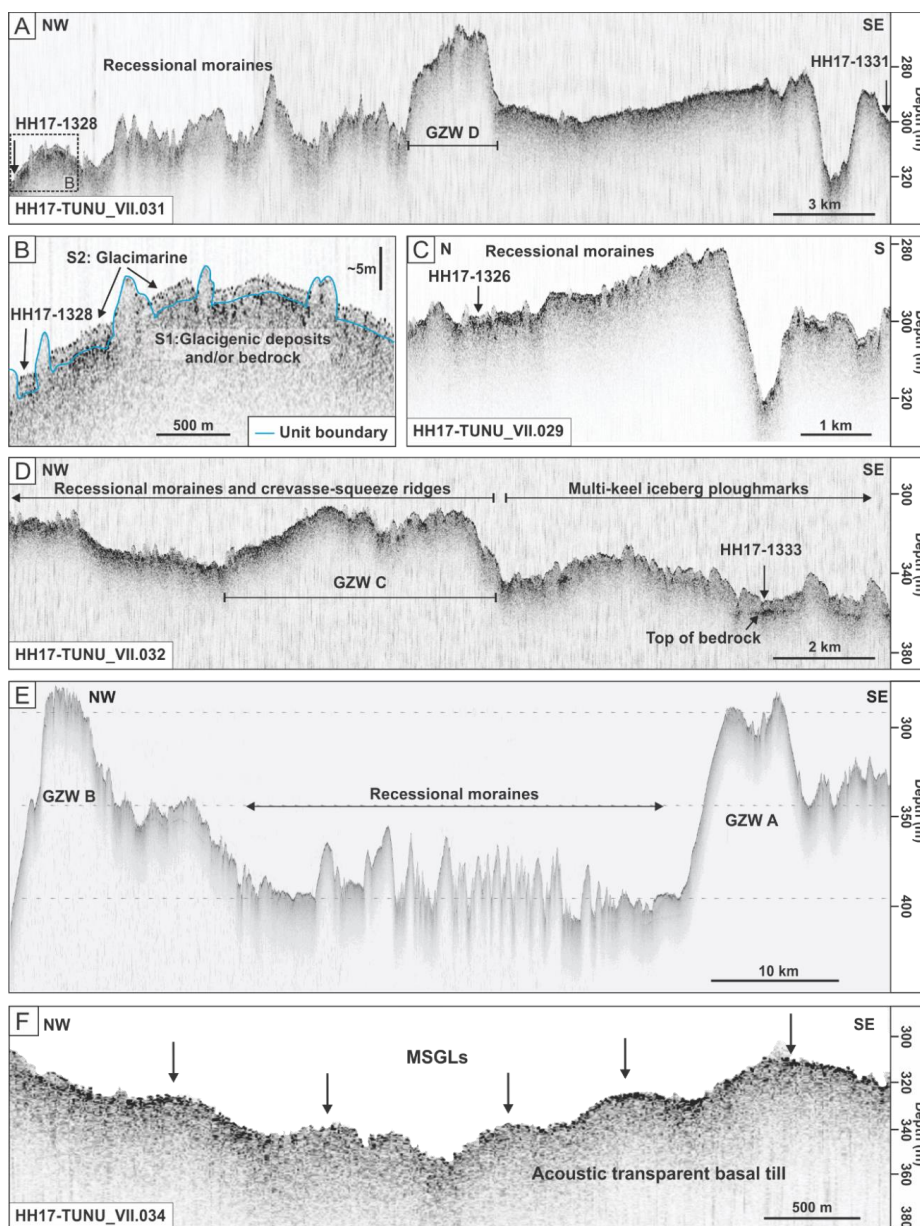


Figure 7. Acoustic profiles from Store Koldewey Trough. See Fig. 1C for locations. (A) Chirp line HH17-TUNU_VII.031 across grounding zone wedge D and recessional moraines from the middle trough area. The approximate positions of sediment cores HH17-1328 and HH17-1331 are shown. Black dotted rectangle shows extent of the profile in (B). (B) Part of chirp line HH17-TUNU_VII.031 showing a zoom-in example of the configuration of units S1 and S2. (C) Chirp line HH17-TUNU_VII.029 from the inner part of the trough, with recessional moraines. The approximate position of sediment core HH17-1326 is indicated. (D) Chirp line HH17-TUNU_VII.032 across grounding zone wedge C. The locations for recessional moraines and crevasse-squeeze ridges, multi-keel iceberg ploughmarks and sediment core HH17-1333 are indicated. (E) Chirp line across grounding zone wedge A and B, separated by recessional moraines. Modified from Laberg et al. (2017). (F) Part of chirp sub-bottom profile HH17-TUNU_VII.034 showing the acoustically transparent deposits interpreted as basal till/mega-scale glacial lineations. The ridges of the latter are indicated with arrows.

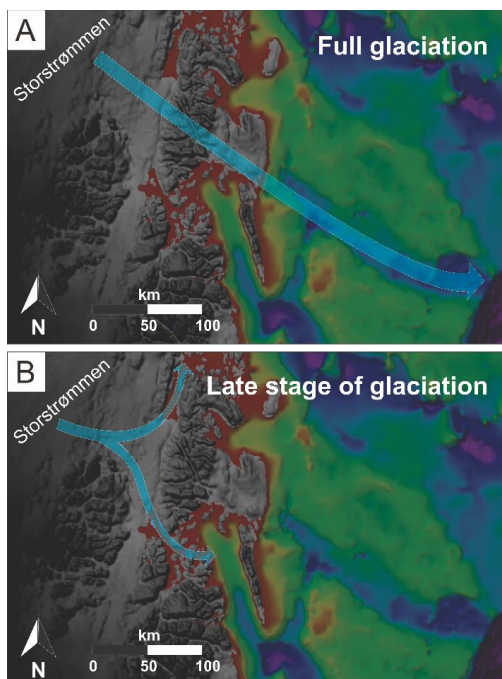


Figure 8. Reconstruction of inferred paleo ice-flow directions showing A) paleo ice-flow unrelated to the underlying topography during full glaciation and B) ice drainage paths during a late stage of glaciation.

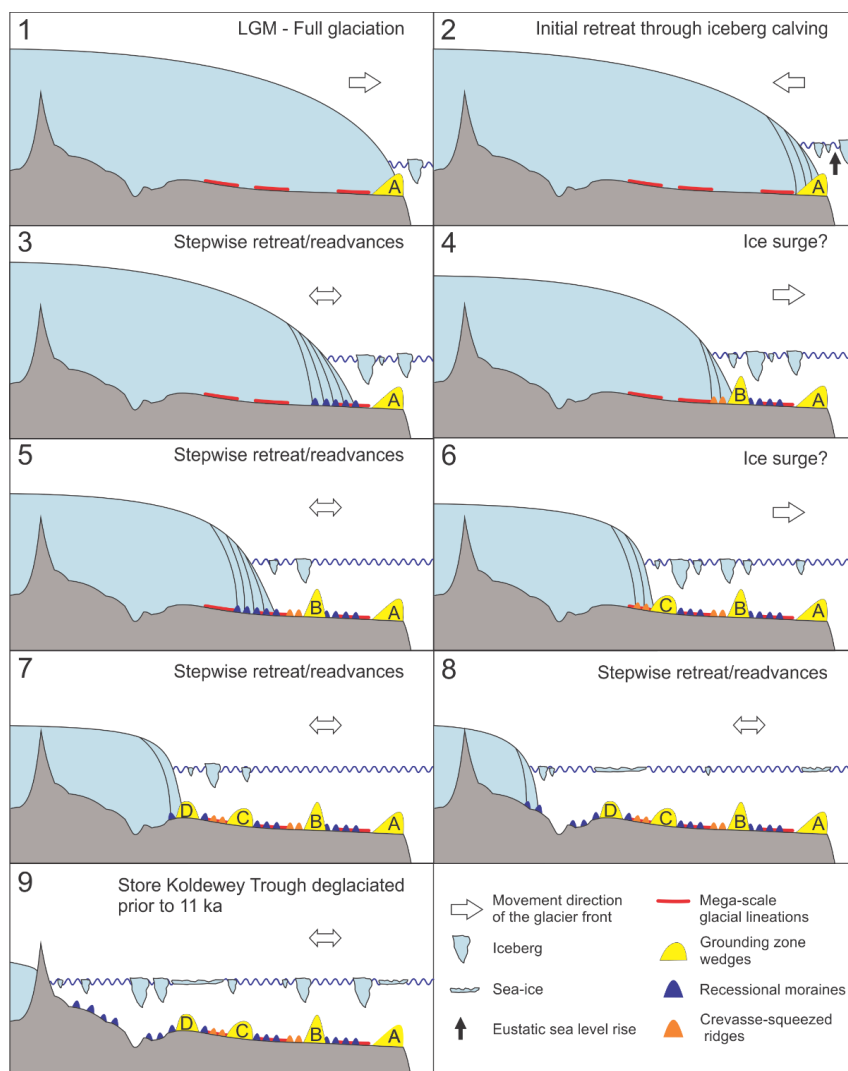


Figure 9. Reconstruction of the ice sheet dynamics in Store Koldewey Trough. Stage 1-9 show the maximum LGM extent of the ice stream, as well as the ice-stream margin positions during the following deglaciation. Icebergs and sea-ice indicate calving and ice rafting. The deglaciation age in stage 9 is based on lake sediment cores on Store Koldewey Ø (Klug et al., 2009).

5

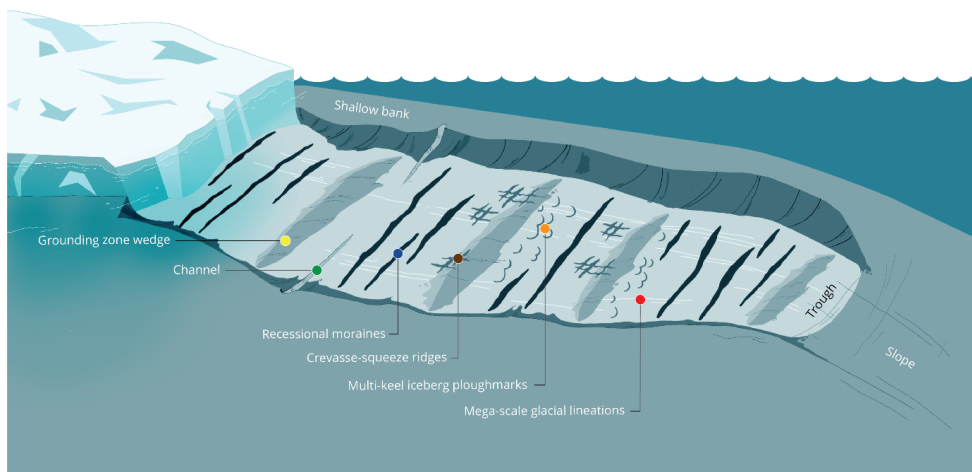


Figure 10. Schematic landform-assemblage model for Store Koldewey Trough.

Core ID	Latitude (°N)	Longitude (°W)	Water depth (m)	Recovery (cm)
HH17-1326-GC-TUNU	76°21.55′	17°05.54′	294	75
HH17-1328-GC-TUNU	76°14.07′	16°05.42′	316	195
HH17-1331-GC-TUNU	76°06.50′	15°07.25′	306	110
HH17-1333-GC-TUNU	76°00.41′	14°09.36′	345	169

5 **Table 1.** Core locations, water depths and recoveries.



Lithofacies	5 - Dmm	4 - Fl	3 - Fl (d)	2 - Fm	1 - Fm (d)
HH17-1326-GC-TUNU (75 cm)	45 cm - end of core	33-45 cm	24-33 cm	12-24 cm	Top of core - 12 cm
HH17-1328-GC-TUNU (195 cm)	152 cm - end of core	117-152 cm	94-117 cm	14-94 cm	Top of core - 14 cm
HH17-1331-GC-TUNU (110 cm)	40 cm - end of core	Absent	26-40 cm	10-20 cm	Top of core - 10 cm 20-26 cm
HH17-1333-GC-TUNU (169 cm)	51 cm - end of core	Absent	33 cm - 51 cm	12-22 cm 28-33 cm	Top of core - 12 cm 22-28 cm
Lithology	Diamicton, massive and matrix-supported with a sandy mud matrix. Randomly oriented clasts	Laminated mud with fine sandy layers	Laminated mud with fine sandy layers and dropstones	Massive mud with rare dropstones	Massive mud with occasional dropstone
Color (Munsell Soil Color Chart)	Very dark gray (2.5Y 3/0)	Dark gray (10YR 4/1)	Dark gray (10YR 4/1)	Olive gray (5Y (2) 4/2) Dark gray (10YR 4/1)	Dark grayish brown (2.5Y 4/2) Dark olive gray (5Y 3/2) Olive gray (5Y (4/2) 4/2) Brown (7.5YR 4/2)
Clast amount	High amounts	Absent	Scattered in layers	Rare	Sections containing clasts
Bioturbation	Absent	Absent	Absent	Little to moderate	Little
Lower unit boundary	Not recovered	Sharp	Gradational or sharp	Gradational	Gradational
Upper unit boundary	Sharp	Gradational	Gradational	Gradational	Top of cores
Bulk density (g/cm ³)	1.61-2.55	1.54-2.03	1.60-2.15	1.60-1.84	1.55-1.78
Magnetic susceptibility (10 ⁻⁵ SI)	20-182	46-148	66-100	53-114	41-106
Shear strength (kPa)	3-52	2-24	2-30	2-14	4-14
Ca/Sum	0.03-0.12	0.04-0.10	0.03-0.07	0.04-0.10	0.03-0.11
Ti/Sum	0.05-0.07	0.05-0.06	0.05-0.07	0.05-0.07	0.03-0.06
Fe/Sum	0.50-0.62	0.55-0.72	0.55-0.70	0.52-0.84	0.52-0.72
Sedimentary environment	Subglacial fill (base of an ice stream)	Proximal glaciomarine sedimentation with suspension plumes and high-density underflows. Ice rafting is absent	Proximal glaciomarine sedimentation with suspension plumes and high-density underflows. Enhanced ice rafting	Distal glaciomarine sedimentation dominated by suspension settling. Ice rafting is limited	Distal glaciomarine sedimentation dominated by suspension settling. Enhanced ice rafting

Table 2. Overview of the main properties and compositional characteristics of the lithofacies, including depositional environment.



	Length (km)	Width (m)	Relief (m)	Spacing (m)
Mega-scale glacial lineations	>1.5	150-500	4-8	200-700
Grounding zone wedges	N/A	3500-10,000	35-100	45,000-60,000
Small ridges	N/A	<2200	<50	50-500
Multi-keel iceberg ploughmarks	<1.3	170-1100	5-30	N/A
Channels	N/A	150-300	3-10	N/A

Table 3. Dimensions of submarine landforms.